Cenomanian to Coniacian Water-mass Evolution in the Cretaceous Western Interior Seaway of North America and Equatorial Atlantic

James S. Eldrett[1], Paul Dodsworth[2], Steven C. Bergman[3], Milly Wright[4]

[1]Shell International Exploration & Production B.V, Kesslerpark 1, 2288 GS Rijswijk, Netherlands.

[2]StrataSolve Ltd, 42 Gaskell Street, Stockton Heath, Warrington, WA4 2UN, UK.

[3]Shell International Exploration and Production Inc, 3333 Highway 6 South, Houston, TX, 77082, USA.

[4]Chemostrat Inc., 3760 Westchase Drive, Houston, Texas, TX 77042. USA.

Correspondence to James S. Eldrett (james.eldrett@shell.com)

Abstract. The Late Cretaceous Epoch was characterized major global perturbations in the carbon cycle, the most prominent occurring near the Cenomanian-Turonian (CT) transition marked by Oceanic Anoxic Event/OAE-2 at 94.9 – 93.7 Ma. The Cretaceous Western Interior Seaway (KWIS) was one of several epicontinental seas in which a complex water-mass evolution was recorded in widespread sedimentary successions. This contribution integrates new data on the main components of organic matter, geochemistry, and stable isotopes along a North-South transect from the KWIS to the equatorial western Atlantic and Southern Ocean. In particular, cored sedimentary rocks from the Eagle Ford Group of West Texas (~90-98 Ma) demonstrate subtle temporal and spatial variations in paleoenvironmental conditions and provide an important geographic constraint for interpreting water-mass evolution. High latitude (boreal-austral), equatorial tethyan and locally sourced Western Interior Seaway water-masses are distinguished by distinct palynological assemblages and geochemical signatures. The northward migration of a tethyan water-mass into the KWIS occurred during the early-middle Cenomanian (98-95 Ma) followed by a major re-organization during the latest Cenomanian-Turonian (95-94 Ma) as a full connection with a northerly- boreal water-mass was established during peak transgression. This oceanographic change promoted de-stratification of the water column and improved oxygenation throughout the KWIS and as far south as the Demerara Rise off Suriname. In addition the recorded decline in redox-sensitive trace metals during the onset of OAE-2 likely reflects a genuine oxygenation event related to open water-mass exchange and may have been complicated by variable contribution of organic matter from different sources (e.g. refractory/terrigenous material), requiring further investigation.

Author Contributions: P.D. conducted palynological analyses; M.W. principal investigator for trace metal analyses; J.E. and S.B. integrated and analysed the datasets; all authors co-wrote the paper.

The authors declare no conflict of interest.

KEYWORDS: Cenomanian, Turonian, palynology, trace metal, anoxia, water-mass, boreal, tethyan

5 COPYRIGHT STATEMENT

1. Introduction

The Late Cretaceous Epoch was characterized by sustained global warming, emplacement of several Large Igneous Provinces (LIPs), global extinctions, global sea-level highstands leading to several epicontinental

10 seaways, and major global perturbations in the carbon cycle termed Oceanic Anoxic Events (OAE's), the most prominent occurring at the Cenomanian-Turonian transition, and termed OAE-2 (Schlanger and Jenkins, 1976). This event is globally recognized by a positive carbon isotope excursion (CIE) reflecting the widespread sequestration of ^{12}C-enriched organic matter in marine sediments under global anoxic conditions (see Jenkyns, 2010 and references therein). Proposed hypotheses for initiation of global anoxia and enhanced carbon

15 sequestration include long term triggers such as changes in ocean circulation and eustatic sea level rise, flooding large areas of continental shelves promoting global stratification and stagnation in greenhouse climates (Erbacher et al. 2001), abrupt episodes of volcanogenic activity and emplacement of large igneous provinces (LIPs; Orth et al. 1993; Snow et al. 2005; Turgeon and Creaser, 2008; Kuroda et al. 2007; Duvivier et al. 2014) releasing large quantities of CO_2 in the atmosphere and increasing delivery of hydrothermally-derived and

20 weathered nutrients into the photic zone enhancing primary production (*e.g*., Adams et al., 2010); or a combination of both (*e.g.,* Kidder and Worsley, 2010). However, increasing evidence indicates a decoupling in the precise timing of the CIE (hence OAE-2) and the location of organic-rich sediment deposition, reflecting that deposition of organic-rich sediment was modulated and ultimately dependent on local and regional processes (basin restriction, water stratification, bottom currents, sediment input) although favoured by global phenomena

25 (sea level change, orbital forcing) (*e.g*., Trabucho-Alexandre et al., 2010). This is particularly apparent within shallow epicontinental seaways such as the southern Cretaceous Western Interior Seaway (KWIS) where parts of the seaway experienced anoxia and recorded organic-rich black shales prior to the OAE-2 interval, and in contrast to other globally recognized sections that recorded organic-rich sediments during the OAE-2 interval (e.g. Plenus Marl and Bonarelli intervals in Europe); the KWIS recorded relatively organic-lean and oxygenated

30 sediments (*e.g*, Meyers, 2007; Eldrett et al., 2014).   Thus, the oceanographic regime of the southern KWIS and its influence on the geologic expression of OAE-2 in this shallow epicontinental sea has been considered unique. It has been proposed that ocean circulation in the KWIS was restricted during the Cenomanian, promoting anoxia due to a sill in the southern gateway (i.e. Texas/Mexico); and that late Cenomanian sea level rise (Greenhorn cyclothem of Kauffman, 1977, 1984) was sufficient to reach a critical sill depth allowing a breach of

35 the southern end of the seaway allowing rapid incursion of warm, normal saline tethyan waters (Arthur and Sageman, 2005). Previous publications have characterized the inflow of tethyan waters at this time by the i)

improved environmental conditions as indicated by the sharp increase in abundance and diversity of
foraminiferal/molluscan and ammonite assemblages reaching far north into the KWIS (McNeil and Caldwell,
1981; Kauffman, 1984, 1985; Eicher and Diner, 1985; Elder, 1985; Leckie et al., 1998; Caldwell et al., 1993;
Kauffman and Caldwell, 1993, Elderbak and Leckie, 2016) and ii) the lithologic transition from organic-rich

5   mudrocks to a highly bioturbated limestone dominated facies (Corbett et al. 2014; Lowery et al. 2014).

The inflow of southern more saline waters into the southern KWIS during the latest Cenomanian has been
proposed to either promote overturning of the water-column or mixing with a northern water-mass resulting in
"caballing" and the production of a third more dense water-mass (Hay et al., 1993; Slingerland et al., 1996). In

10   either scenario, the inflow of tethyan water during OAE-2 cumulated in the abrupt oxygenation of the seafloor as
recorded by development of benthic fauna, termed the benthonic zone (Eicher and Worstell, 1970) or Benthic
Zone (Keller and Pardo, 2004). However, it should be noted that the benthonic/benthic zone in the KWIS has
also been shown to correspond with the equatorial migration of boreal dinoflagellate cyst (dinocyst) taxa (Eldrett
et al. 2014; Van Helmond et al. 2016) and has been correlated with a short-lived climate cooling episode termed

15   the Plenus Cold Event (PCE; Eldrett et al. 2014; Van Helmond et al. 2016; Elderbak and Leckie, 2016), whereby
similarly cool boreal waters invaded northern and central Europe (Jefferies, 1963; Gale and Christensen, 1996;
Voigt et al., 2006; Jarvis et al., 2011). It is therefore difficult to reconcile the late Cenomanian inflow of a warm
tethyan water-mass into the southern KWIS, at a time of global cooling and the southerly migration of boreal
taxa and associated water-mass in the KWIS and Europe. It is plausible that a much more complex

20   oceanographic system existed in the KWIS; such as that modelled by Slingerland et al. (1996) and Kump and
Slingerland (1999), whereby a strong cyclonic gyre developed in the central KWIS drawing both tethyan waters
northward along the eastern margin and boreal waters southward along the western margin of the seaway (see
also discussions in Elderbak and Leckie, 2016).

25   In order to better understand and constrain the nature and timing of water-mass evolution in the southern
gateway to the KWIS, and the associated paleoenvironmental and paleoclimatic processes, this contribution
presents detailed palynological and geochemical analyses within a multidisciplinary framework from the Eagle
Ford Group (Gr.) and bounding formations of the Buda Limestone and Austin Chalk from southwest Texas,
USA. Furthermore, to place the southern gateway of the KWIS into a more supra-regional understanding we also

30   analysed correlative materials from the central KWIS (Portland-1 core, Colorado) and to the south in the
Tropical Atlantic (ODP Leg 207, Demerara Rise) and Southern Ocean (ODP Leg 183, Kerguelen Plateau).

1.1.   Geological Setting

The Eagle Ford Gr. was deposited during the Cenomanian to Turonian across the broad Comanche Platform in

35   the southern intersection of the KWIS and northern Gulf of Mexico, which represented part of the >3,000 km
long foreland basin that formed behind the greater Cordilleran retro-arc fold-and-thrust belt during Late

Mesozoic through Eocene times along the inboard side of the Cordilleran magmatic arc and accreted allochthonous terranes of North America (e.g., Burchfiel et al. 1992; Dickinson, 2004). The regional tectonic setting was influenced during the Cretaceous by the subduction of the conjugate oceanic plateau to the Shatsky Rise (Liu et al., 2010) dynamic topography from the subducting Farallon Plate (Liu, 2014) and thermally

5   subsiding Gulf of Mexico margin, resulting in the development of broad ramp-shelves including the Comanche Platform with reactivated basement structures defining intra-shelf basins, such as the Maverick Basin and structural highs such as the Terrell Arch. The Cenomanian-Turonian Trans-Pecos region was deposited in a distal sediment starved setting >500 km from the nearest shoreline during a locally quiescent tectonic period resulting in stable platform conditions and gradual subsidence ideal for the preservation of mudstones,

10   limestones and bentonites of the Eagle Ford Gr., the underlying Buda Limestone and overlying Austin Chalk (**Figures 1-2**).

1.2.   Previous Palynological Studies

Previous Cenomanian-Turonian palynological studies of the KWIS include those of Brown and Pierce (1962),

15   Christopher (1982), Courtinat (1993), Li and Habib (1996), Cornell (1997), Dodsworth (2000; 2016), Harris and Tocher (2003), Eldrett et al (2014, 2015a, b) and Van Helmond et al. (2016). Brown and Pierce (1962) first reported dinocysts and other palynomorphs from the Eagle Ford Gr. in northeast Texas, whereas terrestrial sporomorphs were recovered from the Woodbine interval of the Eagle Ford Gr. by Christopher (1982). Subsequently, most studies have focused on the central part of the KWIS and in particular the Global boundary

20   Stratotype Section and Point (GSSP, "golden spike") for the base of the Turonian at Rock Canyon, Pueblo, Colorado (e.g., Courtinat, 1993; Li and Habib, 1996; Dodsworth, 2000; Harris and Tocher, 2003). For the southern sector of the KWIS relatively few sections have been published, notably Cornell (1997) reporting diversified mainly gonyaulacacean dinocyst assemblages from the massive limestones of the Buda Formation (Fm.) in Dona Ana County, New Mexico; and more recently Eldrett *et al* (2014) reporting the incursion of boreal

25   dinocysts in the Eagle Ford Gr. during the OAE-2 CIE interval corresponding with improved bottom-water oxygenation. This equatorial migration of the boreal dinocyst complex *Cyclonephelium compactum–C. membraniphorum* has subsequently been recorded across the KWIS and northern Tethys (see Van Helmond et al. 2016). Many of the regional and globally recognized age diagnostic biostratigraphic events encountered in the KWIS were calibrated against an astronomically tuned and geochronologically constrained age model for the

30   Cenomanian-Turonian and early Coniacian based on a relatively expanded section of the Eagle Ford Gr. and bounding units of the Austin Chalk and Buda Limestone that were recovered from the Shell Iona-1 research core, in west Texas (Eldrett et al. 2015a). Paleoenvironmental reconstructions of the Eagle Ford Gr based on the biostratigraphic assemblage data presented by Eldrett et al. (2015a) were beyond the scope of that paper; but some aspects were presented as part of an integrated multidisciplinary contribution demonstrating that obliquity

35   and precession forcing on the latitudinal distribution of solar insolation may have been responsible for the observed lithological and environmental variations through the Cenomanian, Turonian and Coniacian in mid-latitude epicontinental sea settings (Eldrett et al. 2015b). Subsequently, Dodsworth (2016) provided more detailed paleonenvironmental interpretations from palynological assemblages primarily from the Eagle Ford Gr.

exposed at the Lozier Canyon cliff section, Terrell County, west Texas, which is similar to the Innes-1 core (see below) and contains a significant unconformity (duration > 2 myr) within the Turonian. This unconformity is much less intense (duration<0.2myr) in the more distal Iona-1 core.

5   This paper aims to build up and expand these previous contributions by: i) providing detailed palynological interpretations of the Eagle Ford Gr. based on several locations enabling a more widespread geographic understanding; ii) integrating multidisciplinary datasets including organic and inorganic geochemistry allowing a greater understanding of the main paleoenvironmental controls; and iii) presenting new data analysed from sections further to the north in the KWIS (Portland-1 core) and to the south in the Tropical Atlantic (ODP Leg

10   207, Demerara Rise) and Southern Ocean (ODP Leg 183, Kerguelen Plateau) to provide insights into supra-regional ocean circulation and water-mass evolution during the Cenomanian-Turonian Greenhouse climate state.

2. Material & Methods

Core material from the Eagle Ford Gr., and bounding units in the Maverick Basin, West Texas, U.S.A., were

15   analysed for visual kerogen analyses (palynology, palynofacies). The core material was sampled along a physiographic transect from the main Comanche carbonate shelf (Innes-1) towards the edge of the Maverick intra-shelf basin (Iona-1) and central part of the intra-shelf basin (well 'X'). Outcrop sections were also analysed in the San Marcos Arch area near Austin along the Bouldin Creek section. In order to compare data collected from the Eagle Ford Gr., with any regional trends, data were also collected further to the North near the base of

20   the Turonian GSSP (Kennedy et al. 2005; Sageman et al. 2006) in Colorado (USGS Portland-1) and to the South in the Tropical Atlantic off Suriname (ODP Leg 207; Sites 1260 and 1261, Demerara Rise; Shipboard Scientific Party, 2004a, 2004b). Site locations are presented in **Figures 1-2**. Material was also collected from Site 1138, Kerguelen Plateau (Shipboard Scientific Party, 2000). Palynological analyses were conducted under both transmitted and fluorescence microscopy and the results supplemented and compared to newly collected and

25   previously published organic and inorganic geochemical analyses including total organic carbon (TOC) and major, minor and trace elements. Principal Component Analyses (PCA) were run on this integrated dataset to elucidate the primary controls for paleoenvironmental and paleoclimatic interpretations. Details of site locations and methodologies employed are presented in the supplemental information.

30   ## 3. Results
The following section describes some of the key results that are referred to in the discussion section and presented in **Figures 3-11**. Detailed results and data are presented in the supplemental information and datafile.

35

3.1. Organic carbon-isotope Stratigraphy

Significant organic carbon isotopic differences are observed throughout the studied interval. The Buda Limestone record $\delta^{13}C_{org}$ values ~-26‰ and become more negative within the Eagle Ford Gr. where background values are ~-27 to -28‰ for Iona-1, Innes-1 and well 'X'. From these background levels, five notable positive-; and three negative- carbon isotope excursions (CIE) of varying magnitudes were recognized. These excursions can be correlated with the English Chalk reference section of Jarvis et al. (2006; see Eldrett et al. 2015a) and compared with the previously published data for ODP Leg 207 and KWIS as presented in **Figure 3**. Two of these CIE's have specific relevance for this contribution: i) the ~2‰ positive $\delta^{13}C_{org}$ excursion in Iona-1 (143.73m-139.27m) and Innes (76.88m-74.63m) that corresponds with the Middle Cenomanian Event (MCE) and ii) the Cenomanian-Turonian CIE that is clearly expressed with a positive CIE of up to 4‰ occurring in Iona-1 (105.96m-92.73m), Innes-1 (55.74 m- 42.51 m) and well 'X' (1639.9 m – top not recorded as above the cored interval).

3.2. Geochemistry

3.2.1. Southern KWIS (Texas)

The Buda Limestone is characterized in the Iona-1 core by high percentage of calcium oxide (CaO, >45 wt %) and low percentages of Aluminium Oxide (Al_2O_3: <2 wt %), Silica Oxide (SiO_2: <6 wt %) and Titanium Oxide (TiO_2: <1 wt %). Exceptions occur in the interbedded bentonite layers that record higher values of Al_2O_3 (>10 wt %); SiO_2 (>25 wt %) and TiO_2 (~1 wt %). Redox sensitive trace metal concentrations and enrichment factors (EF) in the limestones are low with Molybdenum (Mo); Uranium (U) and Vanadium (V) recording <1ppm/<2 EF; <2ppm/<4 EF and <20ppm/<2 EF respectively. The lower Eagle Ford Gr. is characterized by high TOC and concentrations of redox sensitive trace metals that are enriched compared to average shale. In particular, the basal most part of the lower Eagle Ford Gr. at Iona-1 (153m – 144m) records the highest trace metal enrichments with Mo_{EF} = ave. 400, U_{EF} = 12 and V_{EF} = 17. These trace metal enrichments decline sharply at the base of the MCE interval (143.37m – 142.27m) after which they increase again and become relatively enriched (Mo_{EF} = ave. 140, U_{EF} = 7 and V_{EF} = 13). A similar trend is also recorded in both Innes-1 and well 'X' albeit at overall lower values. In all three cores redox sensitive trace metal concentrations and enrichments start to decline prior to the lower - upper Eagle Ford Gr. boundary. The upper part of the Eagle Ford Gr. is characterized by generally low redox sensitive trace metal concentrations and enrichments in all three cores, with minima associated with the interpreted benthonic foraminiferal zone (see Eldrett et al. 2014). Variations in redox trace metals occur between the limestone-marlstone couplets; with marlstones recording slightly elevated enrichments compared to the limestones (see Eldrett et al. 2015b for details). The uppermost part of the Eagle Ford Gr. (corresponding with the Langtry Member; Mb.) record a slight increase in redox sensitive trace metals in mostly marlstone lithologies in both Innes-1 and Iona-1 cores (**Figures 4-5**). The overlying Austin Chalk is generally not enriched in redox sensitive trace metals with the exception of the interbedded marlstones. The Bouldin Creek outcrop locality was not analysed for geochemistry.

3.2.2. Central KWIS (USGS Portland-1, Colorado)

The Dakota Sandstone and Graneros Shale interval in the USGS Portland-1 core (213m to 175m) is predominantly comprised of high relative concentrations of SiO_2 (ave. ~60 wt %) and Al_2O_3 (ave. ~15 wt %). The Thatcher Limestone interval (~185m) is represented by a single sample that records a slight relative increase
5   in CaO (~8 wt %), but it is likely that this sample does adequately represent or resolve the varied lithological end-members recorded in this interval. A relative increase in CaO is recorded from the base of the Lincoln Shale Mb. to near the top of the Hartland Shale Mb. (175.29m – 150m) reaching up to 25 wt %; and then increase substantially to ~40 wt % CaO marking the lithological break of the base of the Bridge Creek Limestone Mb. (~148.6m).

Throughout the Dakota Sandstone and Graneros Shale intervals the majority of the redox sensitive trace metals record low concentrations and are not significantly enriched compared to average shales (e.g. U, V, Ni, Cu, Zn) and Mo is only slightly enriched (Mo_{EF}= ave. 3; ppm= ave. 4 ppm). Redox sensitive trace metals concentrations increase slightly in the Lincoln Shale Mb. and only become significantly enriched in the Porltand-1 core during
15   the deposition of the Hartland Shale Mb. The overlying Bridge Creek Limestone Mb. and in particular the interval recording the OAE-2 CIE is characterized by an overall reduction in redox sensitive trace metals and lack of significant enrichment. However, variations in enrichment are recorded between the marlstone and limestone couplets of the Bridge Creek Limestone Mb.

20   ### 3.2.3. Demerara Rise (ODP Leg 207, Sites 1260 and 1261).

The pre-OAE-2 sediments recovered from ODP sites 1260 and 1261 record high and variable values of CaO (25-50 wt %); which decline substantially during the OAE-2 interval as SiO_2 values increase with maximum values of 47 wt % and 23 wt % recorded for each site respectively (see supplemental datafile). At Site 1260 in the lower part of the studied interval (445.19 and 462.7 meters composite depth; m.c.d) high concentrations of redox
25   sensitive trace metals are recorded that are significantly enriched compared to average shale (see supplemental datafile; **Figure 9**). Concentrations and enrichments of the redox sensitive trace metals decline from these high values around ~443 m.c.d and reach minima during part of the OAE-2 CIE interval (426-423 m.c.d), but still remain enriched compared to average shale (U_{EF} = 10; Mo_{EF} = 25 ; V_{EF} = 4). This same trend is mirrored in the sedimentary record from Site 1261; with minima enrichment values recorded during the OAE-2 CIE interval
30   (albeit in lower resolution) that even though are relatively low compared with the pre-OAE-2 interval are still enriched compared to average shale (minima values: U_{EF} = 12; Mo_{EF} = 46; V_{EF} = 5; **Figure 10**).

3.3. Palynology

Detailed palynological results and data tables are presented in the supplemental dataset and displayed in **Figures**
35   **4-11**.

4. Discussion

4.1. Principal Component Analyses (PCA)

In order to provide additional understanding into the main controls on organic matter composition and paleoenvironmental significance, PCA was conducted on the palynological and geochemical datasets separately

5   and then on the integrated palynological and geochemical dataset. All three analyses showed the similar principal components and clusters and in support of the discussion only the PCA results run on the combined dataset are presented. The combined dataset PCA was run on cores that had multiple detailed analyses from the same core sample/depth, including Innes-1, Iona-1, well 'X', USGS Portland-1 and ODP Sites 1260 and 1261 using the statistical software C2 (http://www.staff.ncl.ac.uk/stephen.juggins/software/C2Home.htm). Variables

10 within the dataset include palynology, major and trace elements, $\delta^{13}C_{org}$ and TOC. The PCA results show a clear grouping of samples along the two primary axes (**Figure 12**).

Eight groups were identified and are stratigraphically defined: Group I = lower Eagle Ford; Group II = upper Eagle Ford; Group III = Buda Limestone and Austin Chalk; Group IV = Bridge Creek Limestone; Group V=

15 Hartland Shale Mb.; Group VI =Graneros Shale; Group VII = Dakota Sandstone and Group VIII = Demerara Rise. Along the principle axis/eigen score 1, samples with high negative scores comprise high CaO contents and are associated with the Buda Limestone and Austin Chalk formations, whereas high positive scores correspond with high values of elements enriched in heavy minerals (Zirconium-Hafnium; Zr-Hf), silicates (quartz, feldspar), clays (Potassium Oxide- Rubidium; K_2O-Rb [illite/k-feldspar], Gallium (Ga)-Al_2O_3 [kaolinite]) and

20 increased terrigenous contributions (T:M ratio) corresponding with the clastics of the Dakota Sandstone Gr. The high positive score along axis 1 may not solely represent terrestrial/detrital riverine dilution, but also reflect diagenetic alteration of the volcanic ash (SiO_2 and heavy minerals) into smectite–illite (see Eldrett et al. 2015b). Therefore, the clustering of the environmental variables along the Axis/Eigen score 1 is interpreted as representing the carbonate - non carbonate/volcaniclastic mixing trend.

Axis/Eigen score 2 is interpreted to represent a restricted/eutrophic/anoxic to open marine/oligotrophic/oxic marine trend with high positive scores associated with high values in TOC, redox sensitive trace metal concentrations and associated with preservation of AOM and prasinophyte algae. It is also noted that high eigen scores are associated with dinocyst assemblages dominated by peridinioid (P-) cysts and particularly taxa

30 comparable to those informally described from Tarfaya, Morocco by Prauss (2012a, b); *Bosedinia cf.* sp 1 & 3 of Prauss (2012b) (photographic illustrations are provided in the supplemental information). Sporadically common/abundant occurrences of *Bosedinia* sp. 1 & sp. 3 were recorded in the Cenomanian and Turonian of Tarfaya by Prauss (2012a, b), where it is often associated with common occurrences of the colonial green alga *Botryococcus*; high concentrations of *Botryococcus* had previously only been reported from fresh/brackish-water

35 paleoenvrinomnets (e.g. Zippi, 1988) and this led Prauss to infer a freshwater affinity for the *Bosedinia*, suggesting it probably represents episodic salinity stratification in the marine paleoenvironment at Tarfaya (Prauss, 2012c). However, in all the localities investigated in this study and also Lozier Canyon (Dodsworth,

2016), abundances of *Bosedinia* cf. sp 1 & 3 are not associated with an increase in *Botryococcus* or terrigenous pollen and spores, or with the presence of fresh-water algal genera such as *Concentricystes, Ovoidites* (*Schizophacus*)*, Pediastrum* and *Schizosporis*. The latter genera are common components at Cenomanian – Turonian continental to fluvial-deltaic settings in Utah (Akyuz et al., 2016) and east Texas (Dodsworth, 2016).

5   In the present study, the persistent occurrence of these freshwater algal genera are restricted to the Dakota Sandstone in the Portland-1 core where they are associated with the only frequent occurrences of *Botryococcus* and super-abundant (>50%) occurrences of terrigenous spores and pollen reported here. Influxes of *Bosedinia* do not co-occur in any of these proximal KWIS settings. The PCA results presented in this study indicates that *Bosedinia cf.* sp 1 & 3 plots positively along eigen score 2, associated with indicators for eutrophic and anoxic

10   marine conditions; potentially representing the enhanced nitrite/nitrate availability in the photic zone (see Dodsworth, 2016).

The high negative eigen scores along axis 2 correspond with proxies associated with open marine oligotrophic conditions such as gonyaulacoid dinocysts (G-cysts) including *Spiniferites* spp., and *Pterodinium* spp.; the latter

15   shows affinity with modern-day *Impagadinium* spp. which is found in oceanic and open marine conditions (Wall et al. 1977; Zonneveld et al. 2013). High negative eigen scores are also associated with proxies indicative of more oxygenated water conditions such as higher concentration of the redox sensitive trace metal Manganese Oxide (MnO) and foraminiferal test linings. The negative eigen scores are therefore interpreted as representing an open marine, oxygenated and oligotrophic depositional environment.   In addition, it is interesting to note that

20   although phytoclasts plot negatively along eigen axis 2 and may represent a reduced masking effect of AOM during oxygenated conditions (Tyson, 1995); they also plot positively along Eigen score 1 (non-carbonate/volcaniclastic trend) alongside freshwater algae and Areoligeracean dinocysts suggestive of a more nearshore environment (Brinkhuis and Zachariasse 1988; Harker et al. 1990; Li and Habib 1996). In addition, a component of this trend may also represent recycling and transportation of nearshore palynomorphs to more

25   distal environments. The eigen scores are plotted against depth for each of the sites in **Figures 4-11** to further support the paleoenvironmental interpretation as discussed below.

4.2.   Paleoenvironment Interpretation
4.2.1.   Southern KWIS

30   The Buda Limestone (early Cenomanian; ca 98-97.5 Ma) comprises highly diverse and low abundance dinocyst assemblages (see also Cornell, 1997) indicative of open marine oligotrophic conditions. This interpretation is supported by the i) PCA results reflecting the lack of enrichment in redox sensitive trace metals, low TOC and poor preservation of AOM; dominance of G-cysts and ii) sedimentological and micropaleontological evidence for abundant and diverse benthos indicative of a healthy carbonate factory. The Buda Limestone dinocyst

35   assemblages are comparable to those reported from marine limestone facies of early Cenomanian age in western Europe, including England (e.g. Cookson and Hughes, 1964) and France (e.g. Foucher, 1980).

The overlying lower Eagle Ford Gr. interval (ca. 97.2-94.9 Ma) is generally characterized by decline in dinocyst species diversity, with the palynological assemblages comprising high absolute abundance of prasinophyte phycomata with P-cysts being the major component of the dinocyst community indicative of eutrophic and stratified water column conditions. This interpretation is supported by PCA results reflecting the enrichment and

5   co-variance in redox sensitive trace metals and high TOC values combined with low, but sporadic occurrences of benthic foraminifera indicative of restricted and suboxic-anoxic depositional conditions (see also Eldrett et al. 2014). Furthermore, the presence of aryl isoprenoids in the lower Eagle Ford Gr. section from Iona-1 has been demonstrated as originating from *Chlorobi* (green sulphur bacteria) and thus evidence for at least temporary and/or partial photic zone euxinia at this time (Sun et al. 2016). Bed- scale variations are also identified in redox

10   conditions recording greater water-mass ventilation and current activity during the deposition of limestone beds compared to deposition of marlstone beds due to combined obliquity and precessional forcing on solar insolation (Eldrett et al. 2015b). Comparable palynological assemblages have not been reported from the middle to upper Cenomanian deposits in Europe but high relative abundances of prasinophyte phycomata and the peridinioid genus *Bosedinia* have been documented further south in the Cenomanian and Turonian organic-rich shale facies

15   at Tarfaya (Prauss 2012a, 2012b) in north Africa.

Within the middle part of the lower Eagle Ford Gr. (~96.1-95.4 Ma) the relative abundance contribution of prasinophyte phycomata to the palynological assemblage decreases as the absolute abundance of the P-cyst *Bosedinia cf.* sp 1 & 3 significantly increases. This shift in the palynological assemblage is recorded in all the

20   studied sections including the San Marcos Arch outcrop; also in the nearby Lozier Canyon outcrop section (Dodsworth, 2016). As discussed in **section 4.1**, the abundance of *Bosedinia* sp. 1 & sp. 3 had previously been interpreted as reflecting the occurrence of freshwater/brackish water conditions in the photic zone at Tarfaya and episodic salinity stratification there (Prauss 2012a, 2012b, 2012c), but in the absence of freshwater algae and the combined PCA results for the studied sections this interpretation is not supported here for the KWIS or

25   Demerara Rise. Alternatively, Dodsworth (2016) proposed that the introduction of waters from respectively deeper denitrification zones into photic zone by vertical expansion of the oxygen-minimum zone or by upwelling may be a controlling factor, with reduced nitrogen/ ammonium favouring prasinophyte algal production (cf. Prauss 2007) and availability of nitrite/nitrate promoting P-cyst (e.g. *Bosedinia* sp. 1 & sp. 3) productivity in the surface waters. In order to resolve the contribution and variation in the nitrogen cycle and its impact on

30   community structure of primary producers stable nitrogen isotope data are currently being acquired and it is the authors' intention to publish this data when available.

The upper Eagle Ford Gr. associated with first peak ("A") of the OAE-2 CIE (~94.65 Ma) is characterized by a sharp change in palynological assemblages with increase abundance of G-cysts, in particular open marine forms

35   including *Pterodinium*, *Spiniferites ramosus* and *Nematopshaeropsis* spp. Prasinophyte phycomata become rare and overall dinocyst diversity increases. This assemblage shift along with the reduction in redox sensitive trace metal enrichments; lowered TOC; increased bioturbation and occurrence of benthic foraminifera indicate

deposition within an open marine meso-oligotrophic and oxygenated depositional environment (also see Eldrett et al. 2014). By contrast, in some European depositional basins, e.g. eastern England, northern Germany and Crimea, uppermost Cenomanian to lower Turonian deposits associated with OAE-2 are characterized by intervals of interbedded organic-rich shales that contain isolated influxes of prasinophyte phycomata and higher

5   numbers of P-cysts than under- and overlying formations (Marshall and Batten, 1988; Dodsworth, 1996; 2004; Prauss, 2006); whereas limestone deposition is continuous in other areas, e.g. southern England – northern France. The relative increase in the T:M ratio during OAE-2 in the studied sections presented here likely reflects the closed-sum effect as absolute abundance of marine palynomorphs decreases during the upper Eagle Ford (transition from eutrophic to meso-oligotrophic conditions). Absolute abundance of terrestrial palynomorphs

10   does not increase significantly, although this may partly reflect greater distance from shoreline during the Cenomanian-Turonian transgression and potentially diluted concentration of all palynomorphs including pollen during increased biogenic carbonate productivity associated with the limestones of the upper Eagle Ford – Lower Bridge Creek. An increase in absolute abundance of terrestrial palynomorphs is recorded at the Pueblo GSSP, in uppermost Cenomanian beds 82-lower 85 (2000-5000 counts per gram; 30-60%; Dodsworth, 2000). It is unclear

15   whether palynological assemblages in the studied sections support increased hydrological cycle during OAE-2 (see Van Helmond et al. 2014). The sporomorph assemblages during OAE-2 mainly record a relative increase in gymnosperms, in particular during the PCE interval, and thus any increase in T:M ratio may reflect transition from mega-thermal to meso-thermal vegetation (perhaps also reflecting increased pollen production by wind dispersed gymnosperms) in response to climate cooling episode rather than increased hydrologic cycle.

The PCA results indicate occasional anoxia within the upper Eagle Ford Gr. interval; which becomes more persistent in the upper-part of the Langtry Mb. as indicated by slight enrichment in redox sensitive trace metals and palynological assemblages recording reduced dinocyst diversity and enhanced abundances of prasinophyte phycomata. Similar abundance increases in prasinophyte phycomata recorded in the Lozier Canyon outcrop

25   section were thought to represent an artefact of their preferential preservation in weathered material (Dodsworth, 2016), but compared to the regional trends identified in well-preserved core alongside trace metal enrichments (and even in the upper part of the South Bosque Formation at the Bouldin Creek outcrop) indicates that this trend reflects a genuine transition to more restricted and at least partially anoxic depositional environment. The limestones of the Austin Chalk record a return to open marine and oxygenated conditions supported by the PCA

30   results reflecting very diverse dinocyst assemblages, comprised mainly G-cysts with abundant foraminiferal test linings, reduced AOM and no enrichments in redox sensitive trace metals.

4.2.2.   Regional water-mass evolution

In this study we infer three main water-mass properties: i) a restricted suboxic-anoxic marine water-mass

35   characterized by low diversity dinocyst assemblages interpreted to represent a tethyan source; ii) an unrestricted/open marine oxygenated water-mass characterized by high diversity dinocyst assemblages interpreted to represent a boreal source and iii) a partially restricted dysoxic water-mass interpreted to represent a

more local central KWIS source. Comparing the paleoenvironmental trends recorded in the Cenomanian –
Coniacian sections from SW Texas to those recorded further north within the central KWIS (USGS Portland-1;
Pueblo GSSP outcrop) and to the south in the equatorial North Atlantic (ODP sites 1260, 1261, Demerara Rise)
allows an attempt at reconstructing the evolution of these various water-masses (**Figure 13-14**). A discussion of

5   dinocyst and pollen paleo-latitudinal provinicialism across these regions during Cenomanian and Turonian times
is given in the supplemental information.

Lower Cenomanian sediments from the Equatorial Atlantic (ODP Site 1260) are interpreted as being deposited
in a stratified suboxic-anoxic marine environment as indicated by laminated organic rich mudrock deposition

10   and positive PCA-2 scores. This interpretation is consistent with a southern tethyan water-mass and a circulation
controlled nutrient trap fuelling surface water productivity and anoxic depositional environment (Jiménez
Berrocoso et al. 2010; Trabucho-Alexandre, 2010). Further to the North in the southern part of the KWIS, the
early Cenomanian is characterized by the deposition Buda Limestone, which is primarily characterized by well
oxygenated conditions. The first incursion of a tethyan water-mass into southern Texas occurs at 97.2 Ma (t1;

15   **Figure 14**) and is marked by the deposition of the organic rich Eagle Ford Gr., above the Buda submarine
unconformity. In the Central KWIS (Portland-1 core), the early Cenomanian is characterized by relatively
dysoxic depositional conditions, with mixed dinocyst assemblages and high abundance of agglutinated benthic
foraminfera (**Figure 8**) indicative of a Western Interior Seaway source. The initial northward expression of a
tethyan water-mass is only evidenced in the central KWIS during the deposition of the Thatcher Limestone Mb.

20   (ca 96.5-96.6 Ma), with slight increases in prasinophte phycomata, decrease in dinocyst diversity, reduced
benthic foraminfera and supported by the occurrence of ammonites, calcareous nannofossils and planktic
foraminifera with tethyan affinities (see Eicher and Diner, 1985; Cobban, 1993; Hancock et al., 1993, Bralower
and Bergen, 1998). Water-mass characteristics fluctuate during the middle Cenomanian in the Portland-1 core,
but are interpreted as being predominately sourced locally from the Western Interior Seaway as evidenced by

25   relatively low enrichments in redox sensitive trace metals and dominant occurrence of agglutinated foraminifera.
This study is limited by the relatively low sampling resolution from the MCE interval; in order to better resolve
the detail and timing of these paleoceanographic variations higher resolution multi-proxy analyses are required.
In the Portland-1 core there is a clear shift from agglutinated to calcareous benthic foraminfera near the top of
the MCE interval suggestive of a tethyan influence (**Figure 8**). However it is only during the deposition of the

30   middle part of the Lincoln Shale (~95.6 Ma) that abundant prasinophyte phycomata, increased trace metal
enrichments and reduced dinocyst diversity point towards a persistent influence of a tethyan water-mass. These
proxies reach maxima along with the abundance of *Bosedinia cf.* sp. 1 & 3 during the deposition of the Hartland
Shale Mb. (~95 Ma; t2: **Figure 14**) indicating the marine transgression of tethyan waters into the KWIS and
mirrors the 3rd order eustatic Greenhorn Cycle (Kauffman, 1977) reaching the maximum flooding at ~94.7 Ma.

35   The long term (3rd order) trends in water-mass evolution reported here are therefore likely driven by variations in
global eustasy related to regional tectonic and/or mantle plume-lithosphere dynamics associated with the
emplacement of LIPs during this Greenhouse period.

During peak transgression (~94.7 Ma, t3; **Figure 14**) a significant oceanographic re-organization was marked initially by increased bottom-water current activity resulting in widespread hiatal surfaces across the KWIS and with the rapid onset more oligotrophic, oxygenated and open marine conditions. These trends are evidenced by increased diversity of dinocyst assemblages dominated by G-cysts; reduction in trace metals abundances,

5   reduced TOC and increased bioturbation/benthic foraminfera abundances cumulating in the development of the Benthonic/Benthic Oxic Zone (Eicher and Worstell, 1970; Keller and Pardo, 2004). This environmental shift is interpreted to reflect the rapid southward incursion of a northerly sourced water-mass into the central and southern KWIS and is supported by the equatorial migration of boreal dinocyst taxa (Eldrett et al. 2014; Van Helmond et al. 2016), occurring during a period of climate cooling with a minima (3–5°C) during the PCE

10   (Jarvis et al. 2011; Van Helmond et al. 2016; Elderbak and Leckie, 2016). Therefore, the increase in abundance and diversity of foraminiferal/molluscan and ammonite assemblages in the KWIS (McNeil and Caldwell, 1981; Kauffman, 1984, 1985; Eicher and Diner, 1985; Elder, 1985; Leckie et al., 1998; Caldwell et al., 1993; Kauffman and Caldwell, 1993, Elderbak and Leckie, 2016) and the lithologic transition from organic-rich mudrocks to limestone dominated facies (Corbett et al. 2014; Lowery et al. 2014) in the latest Cenomanian does

15   not reflect the incursion of tethyan water, but instead the southward flow of a boreal water-mass at this time. Comparable dinocyst assemblages including diversified G-cysts are recorded i) in the Canadian KWIS throughout the Cenomanian and Turonian (e.g. Singh, 1983; Bloch et al. 1999), albeit with higher numbers of boreal P-cyst taxa including *Isabelidinium magnum* and *Eurydinium glomeratum*, and ii) coeval sediments from European shelf (e.g. Foucher, 1980; Jarvis et al. 1988, 2011; Fitzpatrick, 1995; Pearce et al. 2003, 2009; Lignum

20   2009) which also correspond with the influx of boreal macro-fauna (Jefferies, 1962, 1963; Gale and Christensen, 1996; Voigt et al., 2006; Jarvis et al., 2011). Evidence for the southward incursion of a northerly sourced water-mass during the latest Cenomanian is recorded in all the studied sections spanning the central and eastern part of the KWIS and therefore does not support a more complex oceanographic system such as that modelled by Slingerland et al. (1996) and Kump and Slingerland (1999). The data presented here indicates that the initial

25   inflow of tethyan water across the southern gateway is completely replaced by the almost simultaneous southward flow of boreal water (see also Van Helmond et al. 2016), with no evidence for a contemporaneously counter-flowing tethyan water-mass along the eastern margin. However, based on the limited geographic extent of the studied sections these findings are considered tentative, with additional palynological and geochemical investigations on the eastern margin of the KWIS being required to constrain the lateral variability in possible

30   water-mass properties.

Although the migration of boreal dinocyst taxa (namely the *Cyclonephelium compactum–membraniphorum* morphological plexus; van Helmond et al. 2016) during the PCE is not recorded further to the south in the equatorial North Atlantic; a similar shift in palynological assemblages, including a marked decline in

35   prasinophyte algae, is recorded in the shallower shelf settings on Demerara Rise (ODP Site 1261). Furthermore, at ODP Site 1261, the recorded shift towards a more diverse and open-marine dinocyst assemblage is also associated with an increase in the abundance of organic foraminiferal test linings; re-population by calcareous benthic foraminifera (Friedrich et al., 2011), which combined with a reduction in redox sensitive trace metals is indicative of an improvement in environmental conditions and a reduction on the oxygen minimum zone. This

shift in environmental conditions also corresponds with a sea surface temperature minimum in the lower part of the OAE-2 CIE (up to 4°C; Forster et al. 2007) on the flank of Demerara Rise (ODP Site 1260) and perhaps marks the southernmost influence of a boreal water-mass. However, in Site 1260 *Bosedinia cf.* sp.1 & 3 remains abundant despite the decline in prasinophyte algae, redox trace metals and associated increase in benthic

5   foraminifera indicating more complex interaction between water-masses and the oxygen minimum zone along the slope. The southern expression of this boreal influence is therefore limited in duration and extent, mostly affecting shallower water settings. These findings are consistent with Neodymium (Nd) isotope data from Demerara Rise indicative of circulation pattern change in the Atlantic- Tethys at this time (Zheng et al., 2016; Martin et al 2012).

The early Turonian to Coniacian (~94 Ma – 89 Ma, t4-t5: **Figure 14**) is characterized by two further proposed incursions of both boreal and tethyan water into the KWIS. The first Turonian incursion of boreal water into the southern KWIS (~92.5 Ma) was marked by increased bottom water currents and a 125-210 kyr hiatal interval in Iona-1 (Eldrett et al. 2015a, b). This hiatal interval correlates with that of much greater duration in shallower

15   shelf setting of Innes-1 (> 2 myr) and is coeval with the regional middle-lower Turonian hiatus identified throughout the KWIS (e.g. Ewing, 2013). In the central KWIS, at the Pueblo GSSP, the upper part of the lower Turonian and lower part of the middle Turonian substages contain a marked increase in the boreal P-cyst taxa *Isabelidinium magnum* and *Eurydinium glomeratum.* The most notable incursion of tethyan water in Texas in the Turonian corresponds with the Langtry Mb. of the Eagle Ford Gr. and is characterized by greater abundance of

20   prasinophyte phycomata; greater dinocyst P: G ratio; reduced dinocyst diversity; enrichments in redox sensitive trace metals and enhanced preservation of TOC: all indicative of increased surface water organic matter production and preservation due to anoxic bottom-water or sediment-water conditions. The second main incursion of boreal water into Texas occurs in the Turonian-Coniacian and is marked by the development of chalk facies (e.g. Austin Chalk), diverse dinocyst assemblages and a reduction in redox sensitive trace metals

25   and TOC indicative of oxygenated and oligotrophic marine conditions. Although, the transition from the Eagle Ford Gr., to Austin Chalk is conformable in both Iona-1 and Innes-1, an unconformity is identified on the San Marcos Arch (Lowery et al., 2014; this study). Therefore, the major unconformities identified throughout the KWIS also appear to be associated with increased bottom-water current activity linked to regional incursions of boreal water that ventilated the seaway rather than solely by global eustatic drivers that are difficult to reconcile

30   with a greenhouse world without significant polar ice. The development of coeval hiatal intervals are also recorded near the top and base of the OAE-2 CIE in the Bonarelli interval, Italy, where vigorous bottom currents were proposed to be induced by warm and dense saline deep waters originated on tropical shelves in the Tethys and/or proto-Atlantic Ocean (Gambacorta et al. 2016). Although our contribution proposes an alternative mechanism for invigorated circulation, it further supports the suggestion by Gambacorta et al. (2016) that

35   enhanced current activity and associated oceanographic circulation was much more dynamic than previously thought during times of Greenhouse climates when conditions were thought to be more equitable.

4.2.3. Global trace metal draw-down during OAE-2

During the Cenomanian, sediments that have been influenced by tethyan waters record redox sensitive trace metals that are enriched compared to average shale, in particular Molybdenum (Mo) which requires free H_2S (Helz et al. 1996) and is interpreted as reflecting anoxic to euxinic depositional conditions favouring organic

5   matter preservation. The relative enrichment of Mo compared to the other redox elements such as U and V in the pre-OAE-2 lower Eagle Ford Gr., suggests an active cycling of Mn–Fe particulates (especially Mn-oxyhydroxides) between the water column and sediment water interface characteristic of a "particulate shuttle" (Algeo and Tribovillard, 2009; Tribovillard et al. 2012; **Figure 15a**). The presence of aryl isoprenoids in this interval from the Iona-1 core also supports at least temporary and partial water column (photic zone) euxinia at

10   this time (Sun et al. 2016).

During the onset of OAE-2 the recorded depletion of sedimentary redox sensitive trace metals has been proposed to reflect the draw-down of the global trace metal sea-water inventory due to sequestration in sediments under expanded anoxic/euxinic conditions (Hetzel et al. 2009; Dickson et al. 2016; Goldberg et al. 2016). These interpretations are based primarily on the exceptionally low Mo/TOC gradients compared to that documented in

15   modern-day anoxic silled marine basins (Algeo and Lyons, 2006), whereby removal of aqueous Mo concentrations under anoxic/euxinic conditions to the sediment is in excess to resupply by inter-basinal transfer of water masses. This contribution also documents exceptionally low Mo/TOC gradients for sediments spanning the OAE-2 interval from Demerara Rise and SW Texas (**Figure 15b**; also see Hetzel et al. 2009; Eldrett et al. 2014 Fig. DR3), but also from those recovered from the upper Eagle Ford Gr., and from the Dakota Sandstone

20   interval from the Portland-1 core (supplemental datafile).

However, there are three main challenges to the application of Mo/TOC gradients to infer global trace metal inventory drawdown during OAE-2. Firstly, during the OAE-2 interval in the KWIS, Demerara Rise and Kerguelen Plateau, the co-variance between Mo and U indicate deposition along the unrestricted open marine trend (**Figure 15a**; also Eldrett et al. 2014); an interpretation supported by the palynological assemblages

25   presented here. Therefore, during the OAE-2 interval, these localities were not subject to significant hydrographic restriction (e.g., silled basins), being deposited instead along continental margins. Thus the application of modern-day Mo/TOC gradients to infer hydrographic restriction and trace metal drawdown for OAE-2 is not valid (see discussion in Algeo and Lyons, 2006).

Secondly, as Mo is mostly incorporated into organic matter, we propose that the various contributions of

30   different types of organic matter would affect Mo/TOC gradients. Whereas sulfurized organic matter is known to enhance Mo uptake by the sediment (Tribovillard et al. 2004), the impact of variable contributions of labile versus refractory organic matter is not well constrained. The palynological analyses presented here demonstrate increased contribution of refractory terrigenous organic matter (>T:M ratio) in the samples with low Mo/TOC values from the KWIS and Demerara Rise (**Figure 15b**). We cannot determine the impact of this observation as

35   the T:M ratio reflects a relatively small proportion of the total organic matter, however further investigation is warranted into the variable origin of the more dominant and relatively unknown component, namely AOM; and whether Mo is preferentially incorporated within different organic matter components.

Thirdly; in all the sections presented here the depletion in redox sensitive trace metals during OAE-2 is either associated with oxygenated depositional conditions, or an improvement in redox state. Therefore the recorded depletion in redox sensitive trace metals, in particular Mo may instead record a genuine environmental response to benthic oxygenation possibly related to the equatorial migration of boreal water-masses promoting water

5   column de-stratification and partial ventilation/re-oxygenation of the surface - intermediate waters.

These challenges were partly addressed by Dickson et al. (2016) who proposed that the recorded low Mo/TOC gradients from Site 1138, Kerguelen Plateau reflected the widespread and global nature of trace-metal depletion during OAE-2 by demonstrating that i) localized oxygenation was also not responsible due to Mo isotope compositions and ii) organic matter type was not a control due to the low abundance of terrigenous material.

10   Palynological investigation of these sediments (this study) confirms the low abundance of terrigenous material at Site 1138. In addition, the dinocyst assemblage recovered from this site is typical of a well-oxygenated boreal equivalent (austral) water-mass with high diversity and abundance of G-cysts, notably *Cyclonephelium compactum- membraniphorum* dinocyst plexus, and outer neritic to open marine taxa such as *Spiniferites ramosus* and *Pterodinium cingulatum*. These findings would suggest deposition under the influence of an

15   oxygenated and open marine/hydrographically unrestricted austral (Southern Hemisphere) surface water-mass on the Kerguelen Plateau; consistent with the relatively low $\delta^{98/95}$Mo values and Mo-U co-variance trends reflecting oxic-suboxic depositional conditions; with at most sulphidic pore-waters (Dickson et al. 2016). Furthermore, conditions at the sediment-water interface were sufficient for the presence of a low diversity, high carbon-flux benthic foraminifera biofacies (Holbourn and Kuhnt, 2002) as also indicated by the rare occurrence of organic

20   linings of benthic foraminifera throughout the OAE-2 interval at Site 1138 (this study). Therefore, in addition to trace metal drawdown as an explanation to reconcile low Mo/TOC gradients and hydrologically unrestricted regime; it is possible that even in the organic-rich laminated sedimentary intervals (i.e. Sites 1138 and 1260) a slight improvement in redox conditions related to the influence of oxygenated high-latitude austral-boreal water-masses, may result in aqueous H_2S concentrations at the sediment- water interface being below the critical

25   threshold for conversion of molybdate to thiomolybdate (Helz et al. 1996), resulting in the observed depletion in Mo sedimentary concentrations and low Mo/TOC gradients during OAE-2.

5.   Conclusions

This palynological and geochemical study within a multidisciplinary approach has provided insights into

30   depositional environments of the Cenomanian-Turonian Eagle Ford Gr. and bounding formations of the Buda Limestone and Austin Chalk from southwest Texas, USA. The study spans a physiographic transect across the Comanchean Shelf from the shallow setting of the San Marcos Arch (AU2); through the main shelf (Innes-1), the slope (Iona-1) to the intra-shelf basin (well X). Furthermore, comparison of the paleoenvironmental trends recorded in the Cenomanian – Coniacian section from SW Texas to those recorded further north within the

35   central KWIS (USGS Portland-1) and to the south in the equatorial North Atlantic (ODP sites 1260, 1261, Demerara Rise) and Kerguelen Plateau (ODP Site 1138) allows the interpretation of the evolution of various water-masses along this north-south transect. The main findings are:

1. High latitude boreal and austral (Northern and Southern Hemisphere) and equatorial tethyan water-masses can be distinguished based on their distinct palynological assemblages and geochemical signatures.

2. The northward flow of a suboxic-anoxic tethyan water-mass into the Western Interior Seaway occurred during the early-middle Cenomanian; followed by a major re-organisation during the latest Cenomanian- Turonian as a full connection with a northerly- boreal water-mass was established during peak transgression. This oceanographic change promoted de-stratification of the water column and improved oxygenation throughout the KWIS and as far south as the Demerara Rise.

3. These long term trends in water-mass evolution are tentatively linked to third order eustatic transgression-regression cycles driven by regional tectonic and/or mantle plume-lithosphere dynamics associated with the emplacement of LIPs during this time as well as shorter term variations in climate (i.e. Plenus Cold Event).

4. Low Mo/TOC ratios in the equatorial North Atlantic in comparison to other oceanic basins during the onset of OAE-2 argue for partial restriction and draw-down of global trace metal sea-water inventories. However, this study demonstrates that the recorded decline in redox-sensitive trace metals during the onset of OAE-2 likely reflect either a genuine oxygenation event related to open water-mass exchange at this time and/or is further complicated by variable contribution of organic matter from different sources (e.g. refractory/terrigenous material) that requires further evaluation.

6. Acknowledgements

This paper used data generated on sediments recovered and curated by the International Ocean Discovery Program. The authors thank Malcolm Jones and PLS Ltd for palynological preparations; Shell Colleagues in particular Daniel Minisini and Iain Prince for technical discussion and internal review and Shell Exploration and Production Inc., for permission to publish.

References

Adams, D.D., Hurtgen, M.T., Sageman, B.B., 2010. Volcanic triggering of a biogeochemical cascade during Oceanic Anoxic Event 2. Nature Geoscience 3 (3), 201-204.

Akyuz, I., Warny, S., Famubode, O., Bhattacharya, J.P. 2016. Palynology of the Turonian Ferron-Notom Sandstone, Utah: Identification of marine flooding surfaces and Milankovitch cycles in subtropical, ever-wet, paralic to non-marine paleoenvironments. Palynology 40: 122-136.

Algeo, T. J., and Lyons, T.W, 2006, Mo–total organic carbon covariation in modern anoxic marine environments: Implications for analysis of paleoredox and paleohydrographic conditions, Paleoceanography, 21, PA1016, doi:10.1029/2004PA001112

Algeo, T.J. & Tribovillard, N. 2009. Environmental analysis of paleoceanographic systems based on molybdenum-uranium covariation. Chemical Geology, v. 268, p. 211–225.

Arthur, M.A., Sageman, B.B., 2005. Sea level control on source rock development: perspectives from the Holocene Black Sea, the mid-Cretaceous Western Interior Basin of North America, and the Late Devonian Appalachian Basin. In: Harris, N.B. (Ed.), The Deposition of Organic Carbon-rich Sediments: Models, Mechanisms and Consequences. Society for Sedimentary Geology, Tulsa, pp. 35–59.

Bloch, J.D., Schroder-Adams, C.J., Leckie, D.A., Craig, J., McIntyre, D.J. 1999. Sedimentology, micropaleontology, geochemistry, and hydrocarbon potential of shale from the Cretaceous Lower Colorado Group in western Canada. Geological Survey of Canada, Bulletin 531.

Bralower, T.J., Bergen, J.A., 1998. Cenomanian–Santonian calcareous nannofossil biostratigraphy of a transect of cores drilled across the Western Interior Seaway. In: Dean, W.E., Arthur, M.A. (Eds.), Stratigraphy and paleoenvironments of the Cretaceous Western Interior Seaway, USA. SEPM Concepts of Sedimentology and Paleontology. 6, pp. 59–77.

Brinkhuis H, Zachariasse WJ. 1988. Dinoflagellate cysts, sea level changes and planktonic foraminifers across the Cretaceous- Tertiary boundary at El Haria, N.W. Tunisia. Mar Micropaleontol. 13:153-191

Brown CW, Pierce RL. 1962. Palynologic correlations in Cretaceous Eagle Ford group, northeast Texas. Bulletin of the American Association of Petroleum Geologists 46:2133-2147.

Burchfiel, B.C., Cowan, D.S and Davis, G.A. 1992. Tectonic overview of the Cordilleran orogeny in the Western United States, in Burchfiel, B.C., Lipman, P.W., and Zoback, M.L., (eds)., The Cordilleran Orogon: Conterminous. U.S Geological Society of America, The Geology of North America, G-3, p. 407-480.

Caldwell, W. G. E., Diner, R., Eicher, D. L., Fowler, S. P., North, B. R., Stelk, C. R., and von Holdt, W. L., 1993, Foraminiferal biostratigraphy of Cretaceous marine cyclothems, in Caldwell, W.G. E., and Kauffman, E. G., eds., Evolution of the Western Interior basin: Geological Association of Canada Special Paper 39, p. 477-520.

Christopher RA. 1982. The occurrence of the Complexiopollis-Atlanopollis zone (Palynomorphs) in the Eagle Ford group (Upper Cretaceous) of Texas. J Paleontol. 56:525-541.

Cobban, W. A., 1993. Diversity and distribution of Late Cretaceous ammonites, Western Interior, United States. In: Caldwell, W. G. E. and Kauffman, E. G., Eds., Evolution of the Western Interior Basin, 435-451. St. John's, NL: The Geological Association of Canada. Special Paper 39.

Cookson, I.C., Hughes, N.F. 1964. Microplankton from the Cambridge Greensand (mid-Cretaceous). Palaeontology 7: 37-59.

Corbett, M.J., Watkins, D.K., Popspichal, J.J., 2014. A quantitative analysis of calcareous nannofossil bioevents of the Late Cretaceous (Late Cenomanian–Coniacian) Western Interior Seaway and their reliability in established zonation schemes. Mar. Micropaleontol. 109, 30–45.

Cornell WC. 1997. Dinoflagellate cysts from the Buda limestone (Cenomanian), Cerro de Cristo Rey, Dona Ana county, New Mexico. Rev Palaeobot Palynol. 98:153-157.

Courtinat B. 1993. The significance of palynofacies fluctuations in the greenhorn formation (Cenomanian-Turonian) of the western interior basin, USA. Mar Micropaleontol. 21:249-257.

Dickson, A. J., Saker-Clark, M., Jenkyns, H. C., Bottini, C., Erba, E., Russo, F., Gorbanenko, O., Naafs, B. D. A., Pancost, R. D., Robinson, S. A., van den Boorn, S. and Idiz, E. (2016), A Southern Hemisphere record of global trace-metal drawdown and orbital modulation of organic-matter burial across the Cenomanian–Turonian boundary (Ocean Drilling Program Site 1138, Kerguelen Plateau). Sedimentology. Accepted Author Manuscript. doi:10.1111/sed.12303

Dickinson, W.R., 2004. Evolution of the North American Cordillera. Annual Reviews of Earth and Planetary
    Science 32, 13-45.

Dodsworth, P. 1996. Stratigraphy, microfossils and depositional environments of the lowermost part of the
    Welton Chalk Formation (late Cenomanian to early Turonian, Cretaceous) in eastern England. Proceedings
    of the Yorkshire Geological Society 51: 45-64.

Dodsworth P. 2000. Trans-Atlantic dinoflagellate cyst stratigraphy across the Cenomanian-Turonian
    (Cretaceous) stage boundary. J Micropalaeontol. 19:69-84.

Dodsworth, P. 2004. The palynology of the Cenomanian - Turonian (Cretaceous) boundary succession at
    Aksudere in Crimea, Ukraine. Palynology 28: 129-141.

Dodsworth, P. 2016. Palynostratigraphy and palaeoenvironments of the Eagle Ford Group (Upper Cretaceous)
    at the Lozier Canyon outcrop reference section, west Texas, USA. Palynology, 40, 3, 357-378.

Du Vivier, A.D.C., Selby, D., Sageman, B.B., Jarvis, I., Gröcke, D.R., and Voigt, S., 2014, Marine 187Os/188Os
    isotope stratigraphy reveals the interaction of volcanism and ocean circulation during Oceanic Anoxic
    Event 2: Earth and Planetary Sci.Letters, v. 389, p. 23–33, doi:10.1016/j.epsl.2013.12.024.

Eicher, D.L., Worstell, P., 1970. Cenomanian and Turonian foraminifera from the Great Plains, United States.
    Micropaleontology 16, 269–324.

Eicher, D.L.,Diner, R., 1985. Foraminifera as indicators of watermass in the Cretaceous Greenhorn Sea, Western
    Interior. In: Pratt, L., Kauffman, E.G., Zelt, F.B. (Eds.), Fine-grained deposits and biofacies of the
    Cretaceous Western Interior Seaway: evidence of cyclic depositional processes. SEPM Annual Mid-year
    Meeting, Field Trip No. 4, pp. 122–134.

Elder, W.P., 1985. Biotic patterns across the Cenomanian-Turonian extinction boundary near Pueblo, Colorado.
    In: Pratt, L.M., Kauffman, E.G., Zelt, F.B. (Eds.), Field Trip Guidebook No. 4, 157e169.

Elderbak,K and Leckie, M.R. 2016. Paleocirculation and foraminiferal assemblages of the Cenomanian–
    Turonian Bridge Creek Limestone bedding couplets: Productivity vs. dilution during OAE2, Cretaceous
    Research, Volume 60, May 2016, Pages 52-77, http://dx.doi.org/10.1016/j.cretres.2015.11.009.

Eldrett, J.S., Minisini, D.,Bergman, S.C., 2014. Decoupling of the carbon cycle during Oceanic Anoxic Event 2.
    Geology http://dx.doi.org/10.1130/G35520.1.

Eldrett, J.S., Ma, C., Bergman, S.C., Lutz, B., Gregory, F.J., Dodsworth, P., Phipps, M., Hardas, P., Minisini, D.,
    Ozkan, A. and Ramezani, J., 2015a. An astronomically calibrated stratigraphy of the Cenomanian,
    Turonian and earliest Coniacian from the Cretaceous Western Interior Seaway, USA: Implications for
    global chronostratigraphy. Cretaceous Research, 56, pp.316-344.

Eldrett, J.S., Ma, C., Bergman, S.C., Ozkan, A., Minisini, D., Lutz, B., Jackett, S.J., Macaulay, C. and Kelly,
    A.E., 2015b. Origin of limestone–marlstone cycles: astronomic forcing of organic-rich sedimentary rocks
    from the Cenomanian to early Coniacian of the Cretaceous Western Interior Seaway, USA. Earth and
    Planetary Science Letters, 423, pp.98-113.

Erbacher, J., Huber, B.T., Norris, R.D., and Markey, M., 2001. Intensified thermohaline stratification as a
    possible cause for an ocean anoxic event in the Cretaceous period. Nature, 409:325–327.

Erbacher, J., Friedrich., Wilson, P.., Birch, H., Mutterlose., 2005. Stable organic carbon isotope stratigraphy
    across Oceanic Anoxic Event 2 of Demerara Rise, western tropical Atlantic. Geochemistry, Geophysics,
    Geosystems, 6(6), 1-9, doi:10.1029/2004GC000850

Ewing, T. 2013. Eagle Ford - Colorado Connection: Cenomanian to Coniacian in Southwestern North America. AAPG Search and Discovery Article #30288.

Fitzpatrick, M.E.J. 1995. Dinoflagellate cyst biostratigraphy of the Turonian (Upper Cretaceous) of southern England. Cretaceous Research 16: 757-791.

5   Forster, A., S. Schouten, K. Moriya, P. A. Wilson, and J. S. Sinninghe Damsté (2007), Tropical warming and intermittent cooling during the Cenomanian/Turonian oceanic anoxic event 2: Sea surface temperature records from the equatorial Atlantic,Paleoceanography, 22, PA1219, doi:10.1029/2006PA001349.

Foucher, J-C. 1980. Dinoflagellés et acritarches dans le Crétacé du Bolonnais. Pp. 233, 288-297, 310-311 in Robaszynski *et al.*, Synthèse biostratigraphique de l'Aptien au Santonien du Boulonnais à partir de sept groups paléontologiques: Foraminifères, nannoplancton, dinoflagellés et macrofaunes – Zonations micropaléontologiques integrées dans le cadre du Crétacé boreal nord-européen. Revue dr Micropaléontologie 22(4) : 195-321; 28 fig.; 20pl.

Friedrich, O., Voigt, S., Kuhnt, T., and Koch, M.J., 2011, Repeated bottom-water oxygenation during OAE 2: Timing and duration of short-lived benthic foraminiferal repopulation events (Wunstorf, northern Germany): Journal of Micropalaeontology, v. 30, p. 119–128.

Friedrich, O., Erbacher, J., Moriya, K., Wilson, P.A. and Kuhnert, H. 2008. Warm saline intermediate waters in the Cretaceous tropical Atlantic Ocean. Nature Geoscience, 1, 453-457.

Gale, A.S., and Christensen, W.K.1996. Occurrence of the 5 belemnite *Actinocamax plenus* in the Cenomanian of SE France and its significance, Bull. Geol. Soc. Den., 43, 68xyge

20   Gambacorta, G., R. Bersezio, H. Weissert, and E. Erba (2016), Onset and demise ofCretaceous oceanic anoxic events: The coupling of surface and bottom oceanic processes in two pelagic basins of the western Tethys, Paleoceanography, 31, 732–757, doi:10.1002/2015PA002922.

Hancock, J. M., Kennedy, W. J. and Cobban, W. A., 1993. A correlation of the Upper Albian to basal Coniacian sequences of northwest Europe, Texas and the United States Western Interior. In: Caldwell, W. G. E. and Kauffman, E. G., Eds., Evolution of the Western Interior Basin, Geological Association of Canada. Special Paper 39, 453-476. St. John's.

Harris A.J, Tocher B.A. 2003. Palaeoenvironmental analysis of late Cretaceous dinoflagellate cyst assemblages using high-resolution sample correlation from the western interior basin, USA. Mar Micropaleontol. 48:127-148.

30   Harker S.D, Gustav S.H, Riley L.A. 1990. Triassic to Cenomanian stratigraphy of the Witch Ground Graben. In: Brooks SJ, Glennie K, editors. Petroleum geology of North-West Europe. London: Graham & Trotman; p. 809-818.

Hay, W.W., Eicher, D.L., Diner, R., 1993. Physical oceanography and water masses of the Cretaceous Western Interior Seaway. In: Caldwell, W.E.G., Kauffman, E.G. (Eds.), Evolution of the Western Interior Basin. Geological Association of Canada Special Paper 39, 297–318.

Helz, G.R., Miller, C.V., Charnock, J.M., Mosselmans, J.F.W., Pattrick, R.A.D., Garner, C.D., and Vaughan, D.J., 1996. Mechanism of molybdenum removal from the sea and its concentration in black shales: EXAFS evidence. Geochimica Cosmochimica Acta, v. 60, p. 3631–3642.Herrle, J.O., C.J. Schröder-Adams, W. Davis, A.T. Pugh, J.M. Galloway, and J. Fath, 2016. Mid-Cretaceous High Arctic
40   stratigraphy, climate, and Oceanic Anoxic Events. Geology, 43, 5, 403–406. doi:10.1130/G36439.1.

Hetzel, A., Böttcher, M. E., Wortmann, U. G. and Brumsack, H., 2009. Paleo-redox conditions during OAE2 reflected in Demerara Rise sediment geochemistry (ODP Leg 207). Palaeogeography Palaeoclimatology Palaeoecology, v. 273, 302-328.

Holbourn, A., and Kuhnt, W. 2002. Cenomanian-Turonian palaeoceanographic change on the Kerguelen Plateau: a comparison with Northern Hemispheere records. Cretaceous Research 23, 333-349.

Goldberg,T., Poulton,S.W., Wagner, T., Kolonic, S.F., Rehkämper, M., 2016. Molybdenum drawdown during Cretaceous Oceanic Anoxic Event 2, Earth and Planetary Science Letters, 440, 81-91, http://dx.doi.org/10.1016/j.epsl.2016.02.006.

Jarvis, I., Carson, G.A., Cooper, K., Hart, M.B., Horne, D., Leary, P.N., Rosenfeld, A., Tocher, B.A. 1988. Chalk microfossil assemblages and the Cenomanian-Turonian (late Cretaceous) oceanic anoxic event, new data from Dover, England. *Cretaceous Research* 9: 3-103

Jarvis, I., Gale, A.S., Jenkyns, H.C., Pearce, M.A., 2006. Secular variation in Late Cretaceous carbon isotopes: a new δ13C carbonate reference curve for the Cenomanian–Campanian (99.6–70.6 Ma). Geol. Mag. 143, 561–608.

Jarvis, I., Lignum, J.S., Gröcke, D.R., Jenkyns, H.C., Pearce, M.A., 2011. Black Shale deposition, atmospheric CO2 drawdown, and cooling during the Cenomanian-Turonian Oceanic Anoxic Event. Paleoceanography 26, PA3201. http://dx.doi.org/10.1029/2010PA002081.

Jefferies, R.P.S. 1962 The palaeoecology of the *Actinocamax plenus* Subzone (lowest Turonian) in the Anglo-Paris Basin, Palaeontology, 4, 609-647.

Jefferies, R.P.S. 1963 The stratigraphy of the *Actinocamax plenus* Subzone (Turonian) in the Anglo-Paris Basin, P. of the Geologist. Assoc., 74, 1-33.

Jenkyns, H.C., 2010. Geochemistry of oceanic anoxic events. Geochemistry Geophysics Geosystems v.11, Q03004. http://dx.doi.org/10.1029/2009GC002788.

Jiménez Berrocoso, A., MacLeod, K.G., Martin, E.E., Bourbon, E., Isaza Londoño, C., Basak, C., 2010. Nutrient trap for the Late Cretaceous organic-rich black shales in the tropical North Atlantic. Geology38, 1111–1114.

Joo, Y.J., Sageman, B.B., 2014. Cenomanian to Campanian carbon isotope chemostratigraphy from the Western Interior Basin, U.S.A. Journal of Sedimentary Research 84, 529-542. http://dx.doi.org/10.2110/jsr.2014.38

Kauffman, E.G., 1977, Geological and biological overview: Western Interior Cretaceous Basin; in E.G. Kauffman, ed; Cretaceous facies, faunas and paleoenvironments across the Western Interior Basin: The Mountain Geologist, v. 14, n. 3, 4, p. 75-100.

Kauffman, E.G., 1984. Paleobiogeography and evolutionary response dynamic in the CretaceousWestern Interior Seaway of North America. In: Westermann, G.E.G. (Ed.), Jurassic–Cretaceous biochronology and paleogeography of North America. Geological Association of Canada Special Paper. 27, pp. 273–306.

Kauffman, E.G., 1985. Cretaceous evolution of the Western Interior Basin of the United States, *in* Pratt, L.M., Kauffman, E.G., Zelt, F.B., eds., Fine-grained Deposits and Biofacies of the Cretaceous Western Interior Seaway: Evidence of Cyclic Sedimentary Processes, Society of Economic Paleontologists and Mineralogists Guidebook 4, ivGuidebook 4, ivnce of Cyclic Sedimenta

Kauffman, E.G.,Caldwell, W.G.E., 1993. The Western Interior Basin in space and time. In: Kauffman, E.G., Caldwell, W.G.E. (Eds.), Evolution of the Western Interior Basin. Geological Association of Canada Special Paper. 39, pp. 1–30.

Keller, G., and Pardo, A., 2004, Age and paleoenvironment of the Cenomanian- Turonian global stratotype
    section and point at Pueblo, Colorado: Marine Micropaleontology, v. 51, p. 95–128,
    doi:10.1016/j.marmicro.2003.08.004

Kenndey, W.J., Walaszczyk, I., Cobban, W.A., Dodsworth, P., Elder, W.P., Gale, A.S., Scott, G.R., Hancock,
    J.M., Voigt, S., Kirkland, J.I. 2005. The Global Boundary Stratotype Section and Point for the base of the
    Turonian Stage of the Cretaceous: Pueblo, Colorado, U.S.A. Episodes 28: 93-104.

Kidder, D.L. and Worsley, T. R. 2010. Phanerozoic Large Igneous Provinces (LIPs), HEATT

    (Haline Euxinic Acidic Thermal Transgression) Episodes, and Mass Extinctions. Palaeogeography, doi:
    10.1016/j.palaeo.2010.05.036.

Kump, L.R., Slingerland, R.L., 1999. Circulation and stratification of the early Turonian Western Interior
    Seaway: sensitivity to a variety of forcings. In: Barrera, E., Johnson, C. (Eds.), Evolution of Cretaceous
    Ocean-Climate System Geological Society of America Special Paper, 332, pp. 181–190.

Kuroda, J., Ogawa, N.O., Tanimizu, M., Coffin, M.F., Tokuyama, H., Kitazato, H. and Ohkouchi, N. 2007.
    Contemporaneous massive subaerial volcanism and late Cretaceous Oceanic Anoxic Event 2. Earth Planet.
    Sci. Lett., 256, 211–223.

Leckie, R.M., Yuretich, R.F., West, O.L.O., Finkelstein, D., Schmidt, M.G., 1998. Paleo-ceanography of the
    southwestern Western Interior Sea during the time of the Cenomanian–Turonian boundary (Late
    Cretaceous). In: Arthur, M.A., Dean, W.E. (Eds.), Stratigraphy and Paleoenvironments of the Cretaceous
    Western Interior Seaway. In: Society of Economic Paleontologists and Mineralogists Concepts in
    Sedimentology and Paleontology, vol.6, pp.101–126.

Li H, Habib D. 1996. Dinoflagellate stratigraphy and its response to sea level change in Cenomanian-Turonian
    sections of the western interior of the United States. Palaios 11:15-30.

Lignum, J.S. 2009. Cenomanian (upper Cretaceous) palynology and chemostratigraphy: Dinoflagellate cysts as
    indicators of palaeoenvironmental and sea-level change, Ph.D thesis, Kingston University London,
    Kingston upon Thames, UK, 582 pp.

Liu L., M Gurnis, M Seton, J Saleeby, RD Muller, JM Jackson, 2010. The role of oceanic plateau subduction in
    the Laramide orogeny, Nature Geoscience 3 (5), 353-357

Liu, L., 2014. Constraining Cretaceous subduction polarity in eastern Pacific from seismic tomography and
    geodynamic modeling. Geophysical Research Letters, 41(22), pp.8029-8036.

Lowery, C.M., Corbett, M.J., Leckie, M., Watkins, D., Romero, A.M., Pramudito, A., 2014. Foraminiferal and
    nannofossil paleoecology and paleoceanography of the CenomanianeTuronian Eagle Ford Shale of
    southern Texas. Palaeogeography, Palaeoclimatology, Palaeoecology 413, 49-65.

Martin, E.E., MacLeod, K.G., Berrocoso, A.J., and Bourbon, E., 2012, Water mass circulation on Demerara Rise
    during the Late Cretaceous based on Nd isotopes: Earth and Planetary Science Letters, v. 327-328, p. 111–
    120, doi:10.1016/j.epsl.2012.01.037.

Marshall, K.L. and Batten, D.J. 1988. Dinoflagellate cyst associations in Cenomanian-Turonian 'Black Shale'
    sequences of northern Europe. Review of Palaeobotany and Palynology 54: 85-103.

McNeil, D.H., Caldwell, W.G.E., 1981. Cretaceous rocks and their foraminifera in the Manitoba escarpment.
    Geological Association of Canada Special Paper, 21. St. John's

Meyers, S.R., 2007. Production and preservation of organic matter: The significance of iron. Paleoceanography 22, PA4211. http://dx.doi.org/10.1029/2006PA001332

Orth, C.J., Attrep, M., Quintana, L.R., Elder, W.P., Kauffman, E.G., Diner, R., and Villamil, T., 1993, Elemental abundance anomalies in the late Cenomanian extinction interval: A search for the source(s): Earth and Planetary Science Letters, v. 117, p. 189–204, doi:10.1016/0012-821X(93)90126-T.

Pearce, M.A., Jarvis, I., Swan, A.R.H., Murphy, A.M., Tocher, B.A., Edmunds, W.M. 2003. Integrating palynological and geochemical data in a new approach to palaeoecological studies: Upper Cretaceous of the Banterwick Barn Chalk borehole, Berkshire, UK. *Marine Micropaleontology* 47: 271-306.

Pearce, M.A., Jarvis, I., Tocher, B.A. 2009. The Cenomanian-Turonian boundary event, OAE2 and palaeoenvironmental change in epicontinental seas: new insights from the dinocyst and geochemical records. *Palaeogeography, Palaeoclimatology, Palaeoecology* 280: 207-234.

Pratt, L.M. and Threlkeld, C.N. 1985. Stratigraphic Significance of 13C/12C Ratios in Mid-Cretaceous Rocks of the Western Interior, U.S.A. The Mesozoic of Middle North America. Eds. D.F. Stott and D.J. Glass. Canadian Society of Petroleum Geologists 9 (1984): 305-312.

Prauss, M. 2006. The Cenomanian/Turonian Boundary Event (CTBE) at Wunstorf, north-west Germany, as reflected by marine palynology. Cretaceous Research 27: 872-886.

Prauss, M. 2007. Availability of reduced nitrogen chemospecies in photic-zone waters as the ultimate cause of fossil prasinophyte prosperity. Palaios 22: 489-499.

Prauss, M.L., 2012a. The Cenomanian/Turonian Boundary Event (CTBE) at Tarfaya, Morocco: palaeoecological aspects as reflected by marine palynology. Cretac. Res.34, 233–256. http://dx.doi.org/10.1016/j.cretres.2011.11.004.

Prauss, M.L., 2012b. The Cenomanian/Turonian Boundary Event (CTBE) at Tarfaya, Morocco, northwest Africa: Eccentricity controlled water column stratification as major factor for total organic carbon (TOC) accumulation: Evidence from marine palynology. Cretaceous Research, 37: 246-260.

Prauss, M.L., 2012c. Potential freshwater dinocysts from marine upper Cenomanian to upper Coniacian strata of Tarfaya, northwest Africa: Three new species of Bosedinia. *Cretaceous Research*, *37*, pp.285-290.

Sageman, B.B., Meyers, S.R., Arthur, M.A. 2006. Orbital timescale for the Cenomanian-Turonian boundary stratotype and OAE II, central Colorado, USA. Geology, 34: 125-128.

Schlanger, S. O., and H. C. Jenkyns, 1976. Cretaceous oceanic anoxic events: Causes and consequences, Geol. Mijnbouw, 55, 179–184.

Shipboard Scientific Party, 2000. Site 1138. *In* Coffin, M.F., Frey, F.A., Wallace, P.J., et al., *Proc. ODP, Init. Repts.,* 183: College Station, TX (Ocean Drilling Program), 1–205. doi:10.2973/odp.proc.ir.183.106.2000

Shipboard Scientific Party, 2004a. Site 1260. *In* Erbacher, J., Mosher, D.C., Malone, M.J., et al., *Proc. ODP, Init. Repts.,* 207: College Station, TX (Ocean Drilling Program), 1–113. doi:10.2973/odp.proc.ir.207.107.2004

Shipboard Scientific Party, 2004b. Site 1261. *In* Erbacher, J., Mosher, D.C., Malone, M.J., et al., *Proc. ODP, Init. Repts.,* 207: College Station, TX (Ocean Drilling Program), 1–103. doi:10.2973/odp.proc.ir.207.108.2004

Singh, C. 1983. Cenomanian microfloras of the Peace River area, northwestern Alberta. Alberta Research Council, Bulletin 44, 317pp.

Slingerland, R., Kump, L.R., Arthur, M.A., Fawcett, P.J., Sageman, B.B., Barron, E.J., 1996. Estuarine circulation in the Turonian Western Interior seaway of North America. Geol. Soc. Am. Bull. 108, 941–952.

Snow, L.J., Duncan, R.A., Bralower, T.J., 2005. Trace element abundances in the Rock Canyon Anticline, Pueblo, Colorado, marine sedimentary section and their relationship to Caribbean plateau construction and Oxygen Anoxic Event 2. Paleoceanography 20, PA3005.

Sun, X., Zhang, T., Sun, Y., Milliken, K.L., Sun, D., Geochemical evidence of organic matter source input and depositional environments in the lower and upper Eagle Ford Formation, south Texas, Organic Geochemistry (2016), doi: http://dx.doi.org/10.1016/j.orggeochem.2016.05.018

Trabucho Alexandre, J., Tuenter, E., Henstra, G.A., van der Zwan, K.J., van de Wal, R.S.W.,Dijkstra, H.A., de Boer, P.L., 2010. The mid-Cretaceous North Atlantic nutrient trap: Black shales and OAEs: Paleoceanography v. 25, PA4201.

Tribovillard, N., Riboulleau, A., Lyons, T., Baudin, F., 2004. Enhanced trapping of molybdenum by sulfurized marine organic matter of marine origin in Mesozoic limestones and shales. Chemical Geology 213 (4), 385–401.

Tribovillard, N., Algeo, T.J., Baudin , F., Riboulleau, A., 2012. Analysis of marine environmental conditions based on molybdenum–uranium covariation—Applications to Mesozoic paleoceanography. Chemical Geology, Volumes 324–325, 46-58, http://dx.doi.org/10.1016/j.chemgeo.2011.09.009.

Turgeon, S.C., Creaser, R.A., 2008. Cretaceous Anoxic Event 2 triggered by a massive magmatic episode. Nature 454, 323–326.

Tyson, R.V. "Sedimentary Organic Matter; Organic Facies and Palynofacies." London, England: Chapman and Hall, 1995. p. 615.

Van Helmond, N.A.G.M., Sluijs, A., Reichart, G.-J., Sinninghe Damsté, J.S., Slomp, C.P., Brinkhuis, H. 2014. A perturbed hydrological cycle during Oceanic Anoxic Event 2. Geology 42(2): 123-126. doi:10.1130/G34929.1

Van Helmond, N. A. G. M., Sluijs, A., Papadomanolaki, N. M., Plint, A. G., Gröcke, D. R., Pearce, M. A., Eldrett, J. S., Trabucho-Alexandre, J., Walaszczyk, I., van de Schootbrugge, B., and Brinkhuis, H. 2016. Equatorward phytoplankton migration during a cold spell within the Late Cretaceous super-greenhouse, Biogeosciences, 13, 2859-2872, doi:10.5194/bg-13-2859-2016.

Voigt, S., Gale, A.S., and Voigt, T. 2006. "Sea-Level Change, Carbon Cycling and Palaeoclimate during the Late Cenomanian of Northwest Europe: An Integrated Palaeoenvironmental Analysis." Cretaceous Research 27.6: 836-858.

Wall, D., Dale, B., Lohmann, G.P., Smith, W.K. 1977. The environment and climatic distribution of dinoflagellate cysts in modern marine sediments from regions in the North and South Atlantic Oceans and adjacent seas. Mar. Micropaleontol., 2, 121–200.

Zheng, X.-Y., Jenkyns, H. C., Gale, A. S., Ward, D. J. and Henderson, G. M. 2016. A climatic control on reorganization of ocean circulation during the mid-Cenomanian event and Cenomanian–Turonian oceanic anoxic event (OAE 2): Nd isotope evidence. *Geology*, 44, 151–154.

Zippi, P.A. 1998. Freshwater algae from the Mattagami Formation (Albian), Ontario: paleoecology, botanical affinities, and systematic taxonomy. Micropaleontology 44 (Suppl. 1): 1-78.

Zonneveld, K. A. F., Marret, F., Versteegh, G. J. M., Bogus, K., Bonnet, S., Bouimetarhan, I., Crouch, E., de Vernal, A., Elshanawany, R., Edwards, L., Esper, O., Forke, S., Grøsfjeld, K., Henry, M., Holzwarth, U.,

Kielt, J.-F., Kim, S.- Y., Ladouceur, S., Ledu, D., Chen, L., Limoges, A., Londeix, L., Lu, S.-H., Mahmoud, M. S., Marino, G., Matsouka, K., Matthiessen, J., Mildenhal, D. C., Mudie, P., Neil, H. L., Pospelova, V., Qi, Y., Radi, T., Richerol, T., Rochon, A., Sangiorgi, F., Solignac, S., Turon, J.-L., Verleye, T., Wang, Y., Wang, Z., and Young, M. 2013. Atlas of modern dinoflagellate cyst distribution based on 2405 data points, Rev. Palaeobot. Palyno., 191, 1– 197, doi:10.1016/j.revpalbo.2012.08.003.
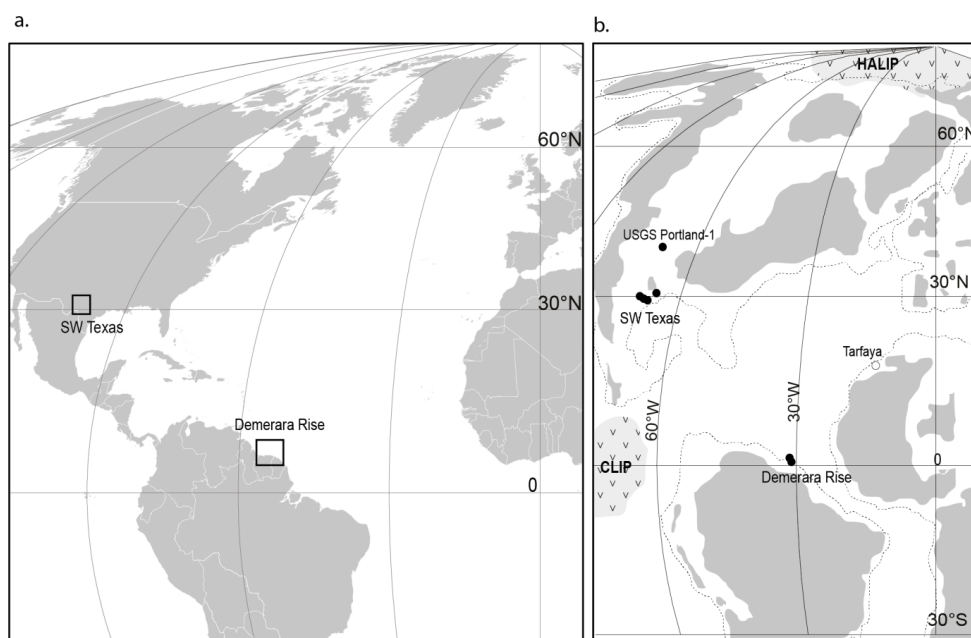
Figure 1: Site Locations. a. Present-day position of the study areas; b. Turonian paleogeographic reconstruction with site locations; gray shaded area= landmass; dotted line = paleo-shelf; CLIP =Caribbean Large Igneous Province; HALIP = High Arctic Large Igneous Province. Boxes show study area as presented in Fig. 2
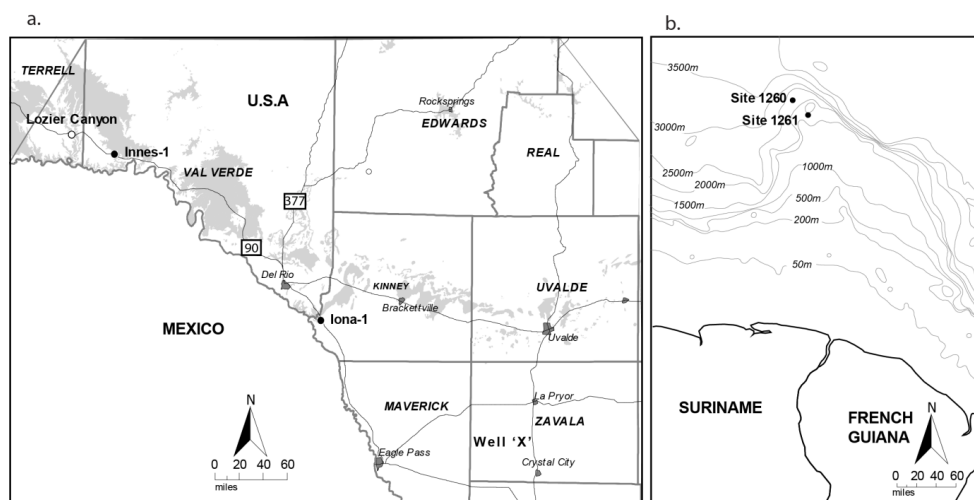
Figure 2: Site Locations. **a.** SW Texas map showing core locations; gray shading = Eagle Ford Gr., outctop belt; **b.** Demerara Rise site locations.
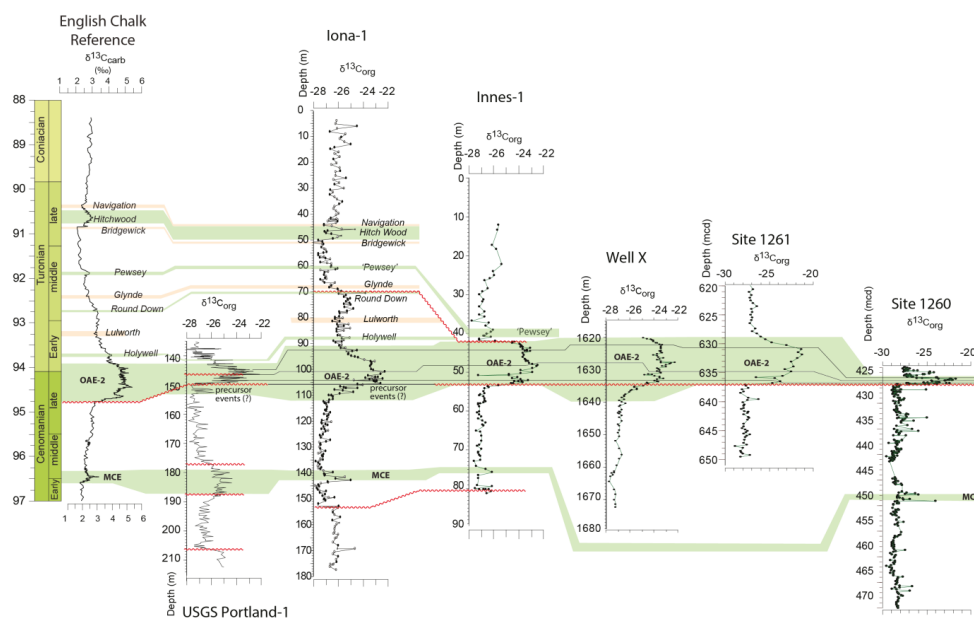
Figure 3: Isotope data and correlation between studied sites and the English Chalk Reference section. Data sources: $\delta^{13}C$ for English Chalk (Jarvis et al. 2006); USGS Portland-1 (Joo and Sageman, 2014; Eldrett et al. 2014; Duvivier et al. 2014; Eldrett et al. 2015a, this study) ODP sites 1260-1261 (Erbacher et al. 2005; Friedrich et al. 2008) Note variable depth scales.
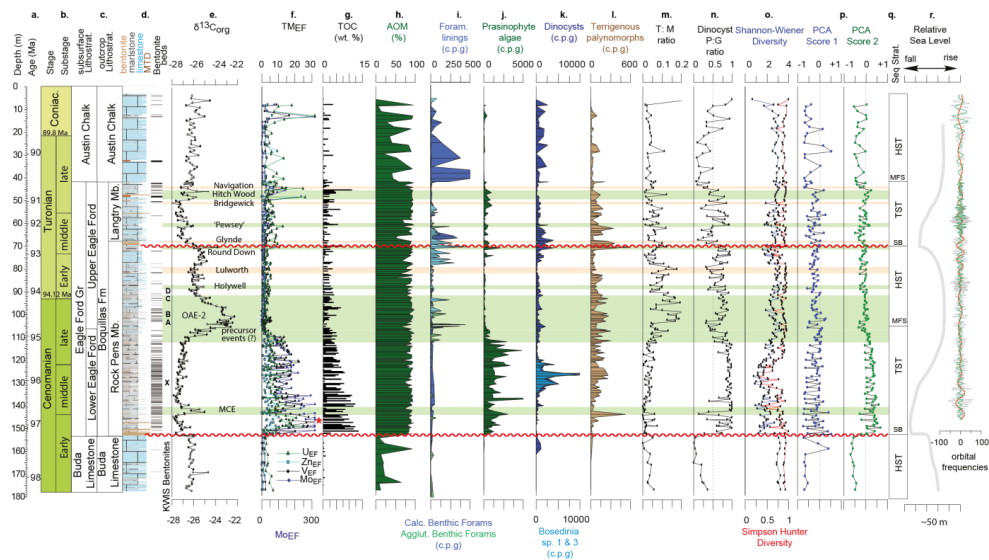
Figure 4: Iona-1 core data. a. depth/age; b. chronostratigraphy; c. lithostratigraphy; d. lithology; e. $\delta^{13}C_{org}$; f. redox sensitive trace metal enrichments (TM_{EF}); g. TOC; h. AOM; i. foraminiferal test linings; micropalaeontological abundance data for benthic foraminifera; j. prasinophyte algae; k. dinocysts, *Bosedinia cf.* sp. 1 & 3; l. Terrigenous palynomorphs; m. T:M ratio; n. dinocyst P:G ratio; o. Shannon-Wiener and Simpson-Hunter dinocyst diversity; p. Principle Component results; eigen score 1, eigen score 2; q. Sequence stratigraphic interpretations; r. inferred relative sea level history with Milankovitch orbital frequencies (after Eldrett et al. 2015a, b).
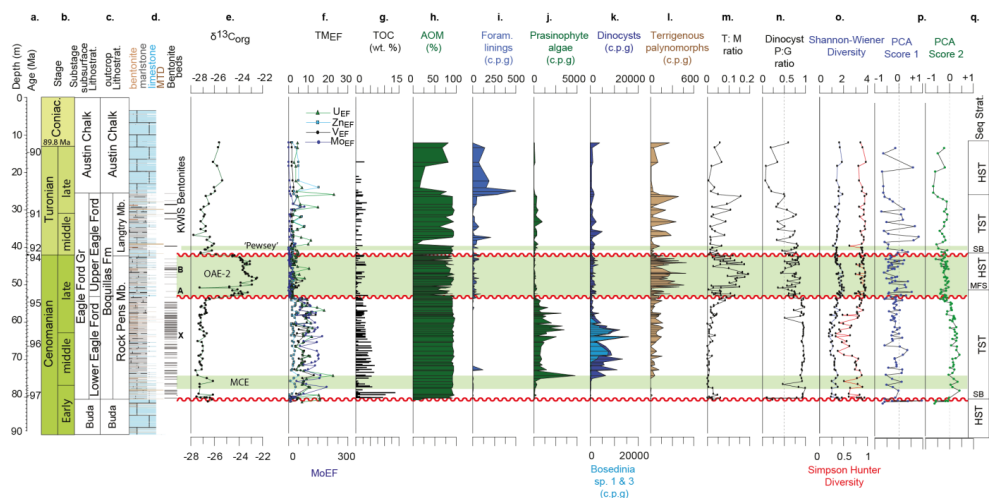
Figure 5: Innes-1 core data. Legend same as Figure 4.
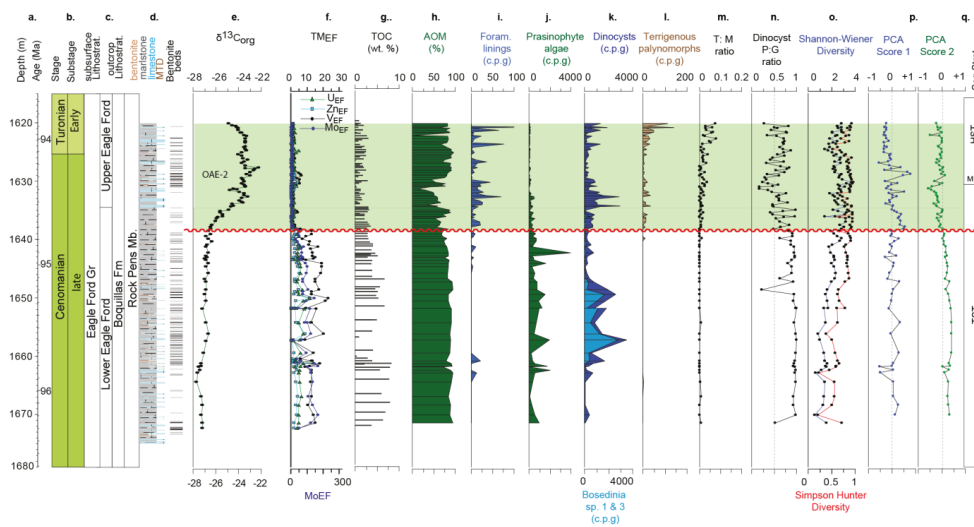
Figure 6: Well 'X' core data. Legend same as Figure 4.
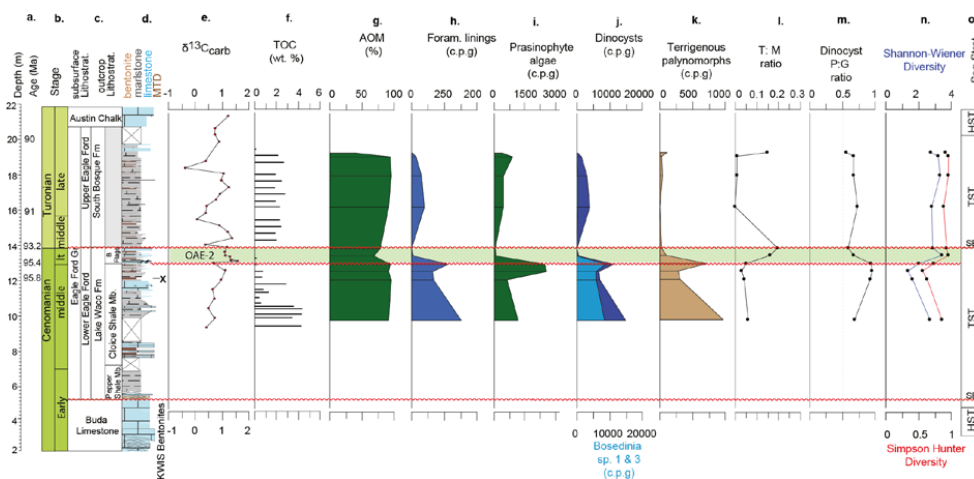
5   **Figure 7:** Bouldin Creek outcrop (AU-2) data. Legend same as Figure 4.
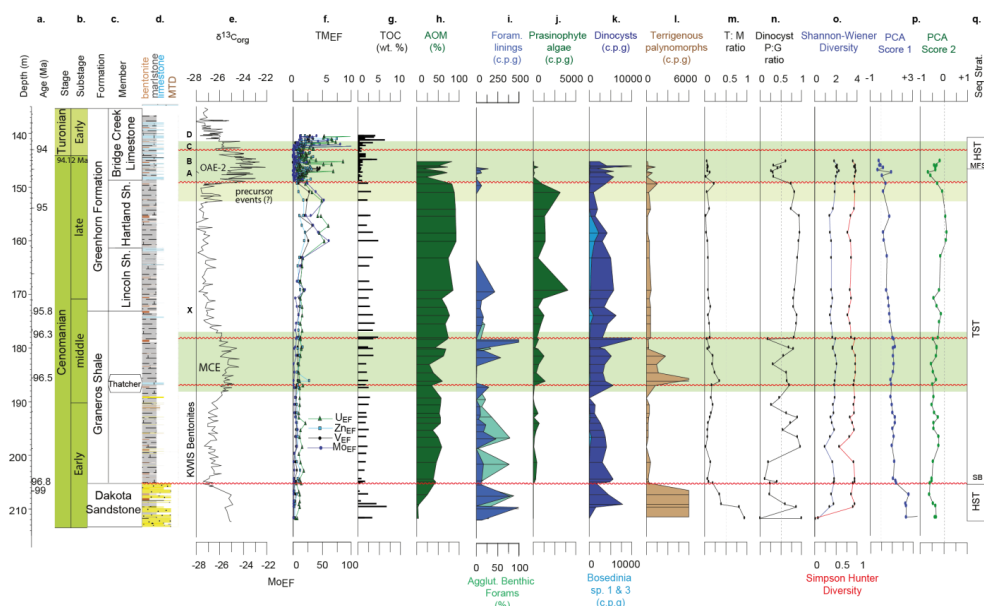
Figure 8: USGS Portland-1 core data. Legend same as Figure 4. δ13Corg data from Joo and Sageman (2014); Eldrett et al. (2014); Duvivier et al. (2014); Eldrett et al. (2015a), this study.
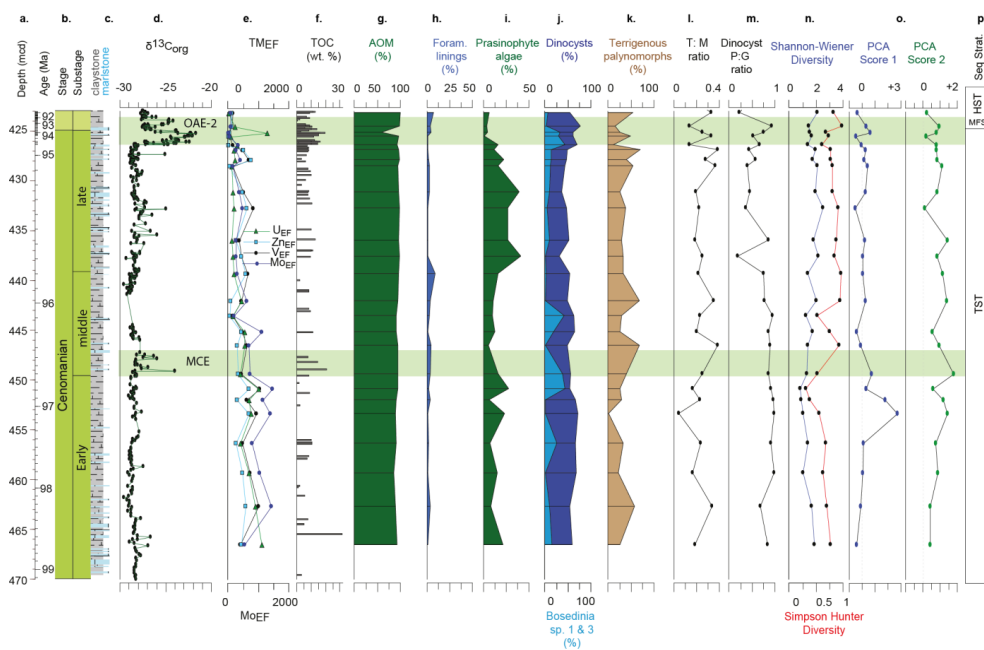
Figure 9: ODP Site 1260 data. Legend same as Figure 4. δ13Corg data from Erbacher et al. (2005); Friedrich et al. (2008).

Figure 10: ODP Site 1261 data. Legend same as Figure 4. $\delta^{13}C_{org}$ data from Erbacher et al. (2005) and Friedrich et al. (2008).
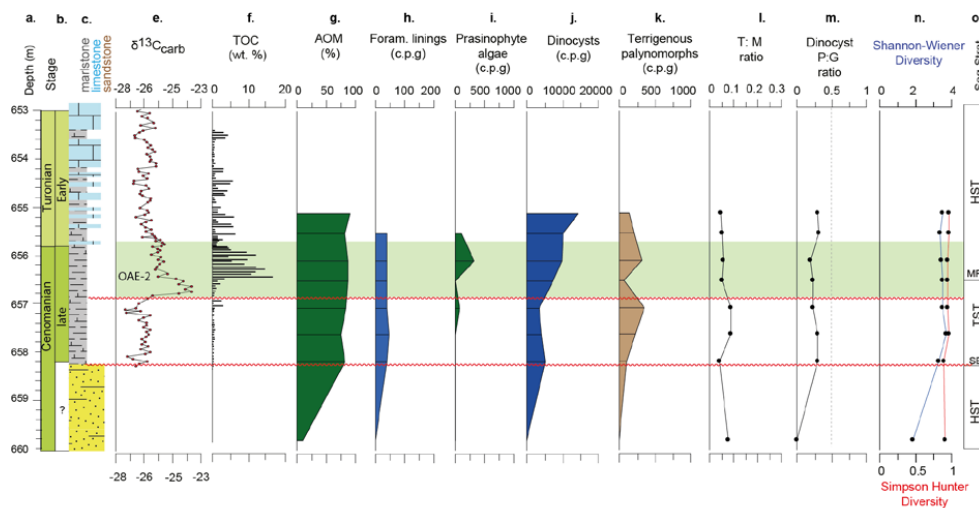
Figure 11: ODP Site 1138 data. Legend same as Figure 4. $\delta^{13}C_{org}$ and TOC data from Dickson et al. (2016).
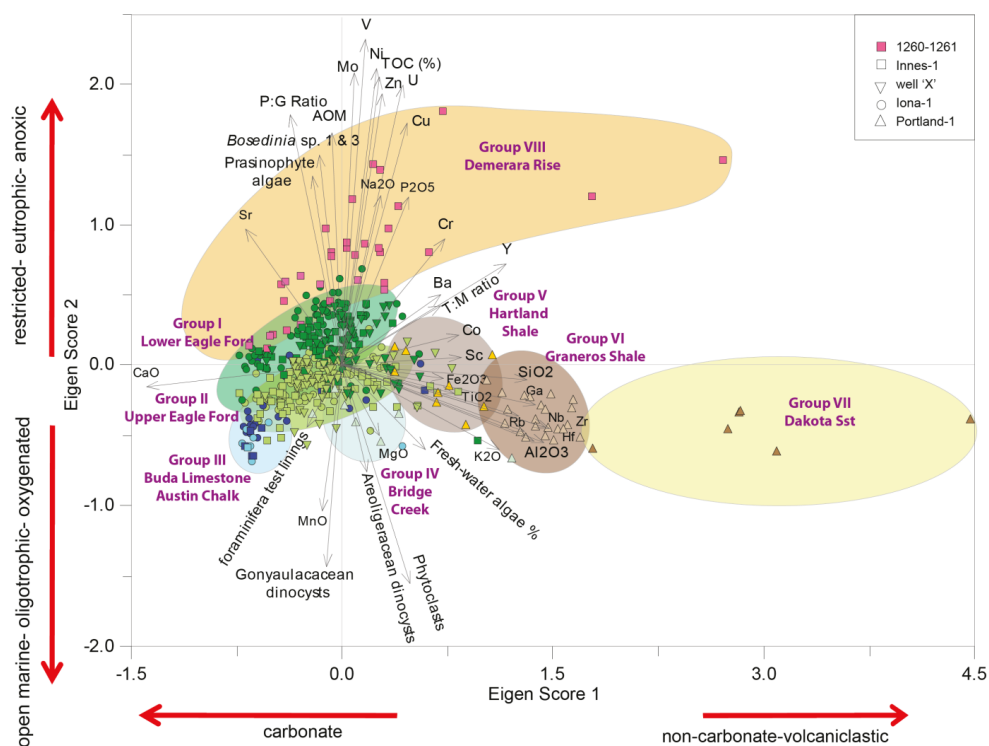
Figure 12: PCA results showing principle axis/eigen scores; selected environmental variables. Samples plotted as a function of site location (see insert) and lithostratigraphic interval (colours; groups in figure).
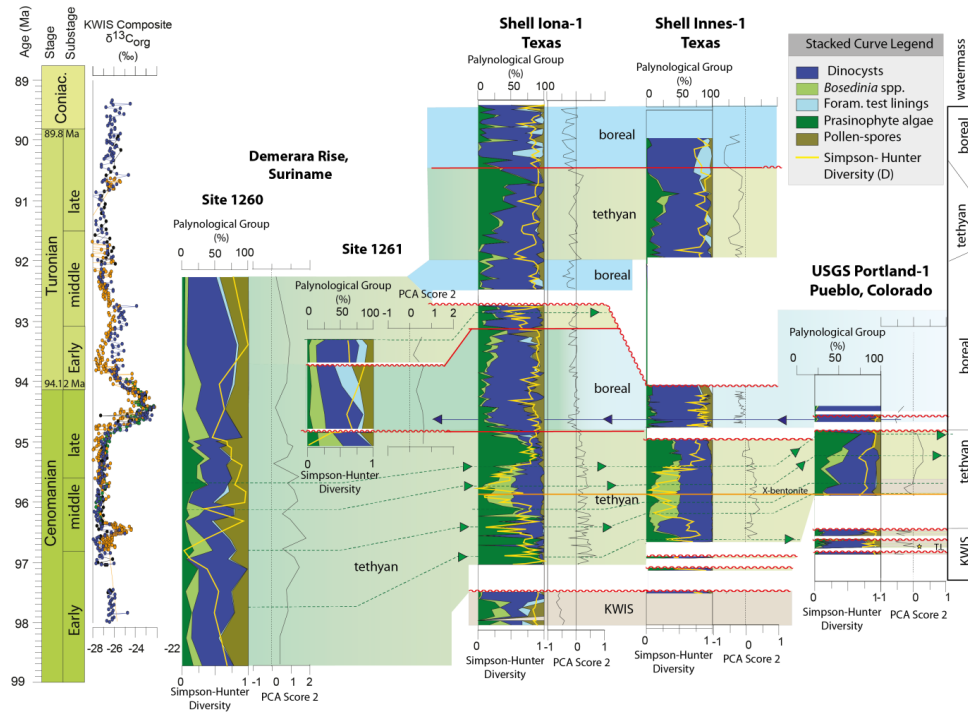
Figure 13: Cenomanian-Coniacian chronostratigraphic correlation of interpreted water-masses along a South-North transect from the equatorial western Atlantic to the central Cretaceous Western Interior Seaway (KWIS). The KWIS composite $\delta^{13}C_{org}$ after Joo and Sageman (2014) and including data from Duvivier et al. (2014), Eldrett et al. (2015) for USGS Portland-1 (orange), plus data from Iona-1 (blue); Innes-1 (black) and well 'X' (green) cores calibrated using the age model of Eldrett et al. (2015a).
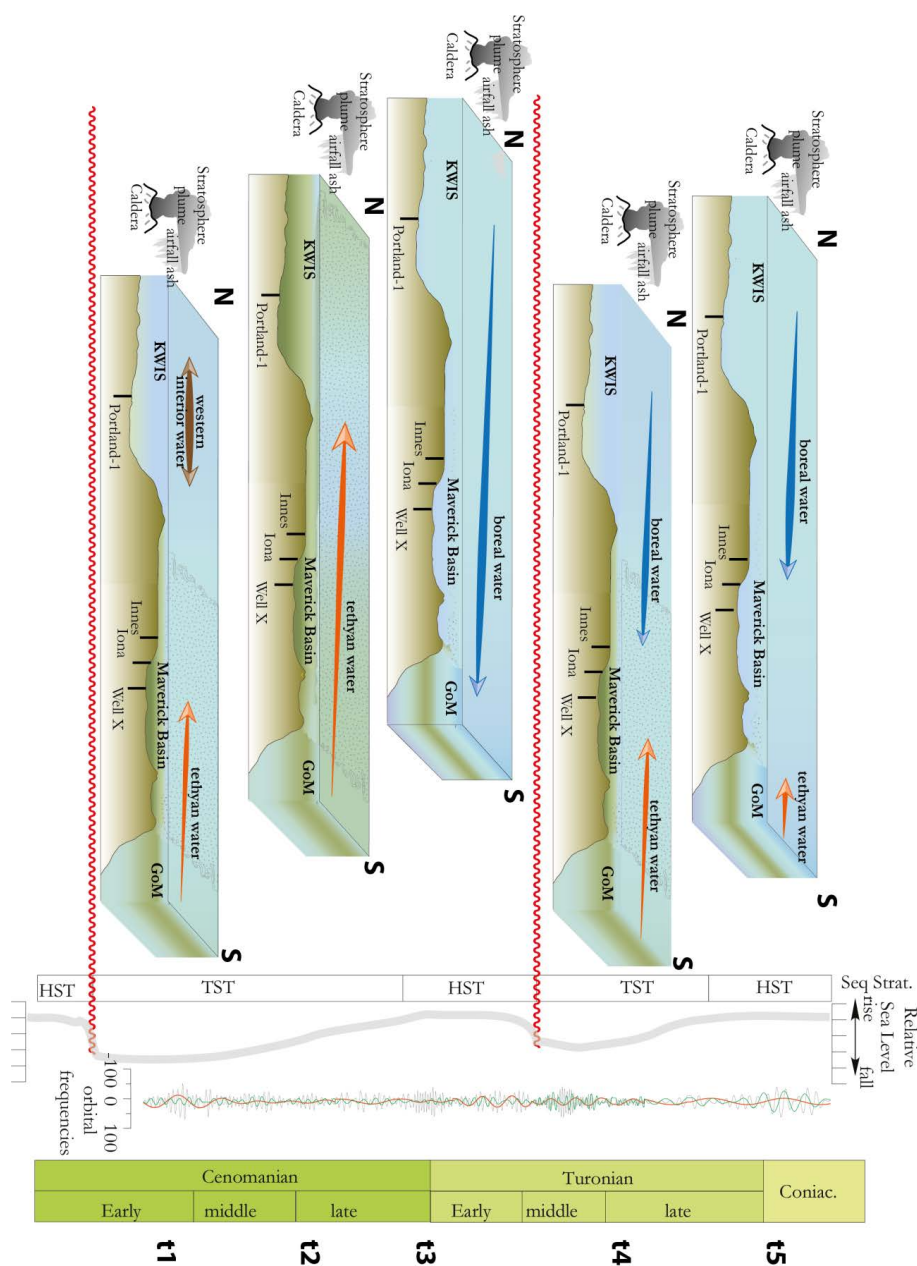
Figure 14. Regional water-mass depositional model of the KWIS. Timesclices (t1-t5) showing the northward flow of eutrophic/anoxic tethyan water into the Western Interior Seaway from the proto-Atlantic and southward flow of a boreal watermass. Milankovitch orbital frequencies of eccentricity, obliquity and precession from the Iona-1 core (Eldrett et al. 2015a) resulting in shorter-term (<0.1 Ma) development of limestone-marlstone couplets (Eldrett et al. 2015b). GoM = Gulf of Mexico.
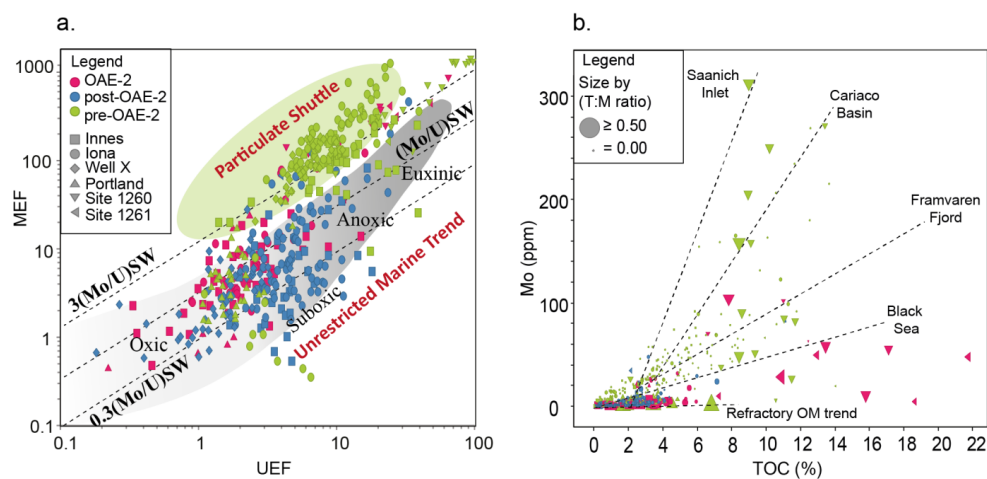
Figure 15. a, Logarithmic plot of Mo:U covariance for the studied sections. Diagonal dashed lines represent multiples (0.3, 1, and 3) of Mo:U ratio (3) of present-day seawater (SW). Values greater than x3 SW are generally associated with the particulate shuttle; whereas those trending with modern day sea water reflect an unrestricted marine trend. **b,** Mo-TOC Covariance data for studied sections compared to modern anoxic silled-basin environments (after Tribovillard et al. 2012).Regression of the modern datasets are shown as solid lines with MO/TOC regression slopes displayed (Tribovillard et al. 2012). The proposed refractory organic matter trend added as dashed line.